Characterizing Intense Pulsed Light-Elicited Effects on *Escherichia coli* and Non-Fat Dry Milk Through Metabolomic and Chemometric Analysis

A THESIS
SUBMITTED TO THE FACULTY OF
UNIVERSITY OF MINNESOTA
BY

QINGQING MAO

IN PARTIAL FULFILLMENT OF THE REQUIREMENTS
FOR THE DEGREE OF
MASTER OF SCIENCE

Advised by Dr. Chi Chen

SEPTEMBER 2019

Acknowledgements

Firstly, I would like to express my sincere gratitude towards my advisor, Dr. Chi Chen. I am very thankful for the unceasing support, guidance, and inspiration throughout the years. His persistent help and teaching make this dissertation a reality. Through the years, Dr. Chen has also kindly shared personal and professional skills, which will for sure be beneficial in my future career. I would also like to thank my committee members: Dr. David Baumler and Dr. Roger Ruan for their advice and inspirations.

I am also grateful for the peer students and principle investigators who have been collaborating on this project: Dr. Roger Ruan, Dr. Paul Chen, Dr. Zata Vickers, Dr. Joellen Feirtag, Dr. Laurence Lee, Dr. David Baumler, Dongjie Chen, Justin Wiertzema, Juer Liu, Peng Peng. The energy channeled in the team makes research more fun and fulfilling.

In addition, many thanks to my lab colleagues, Dana Yao, Lei Wang, Feng Ding, Yiwei Ma, Yuyin Zhou, for their extensive technical support, and the warm and welcoming atmosphere in the lab.

Then, I want to say thank my family and friends, who always selfishly support, encourage, and motivate me to pursue this journey. They build a foundation for me to stand at where I am today.

ABSTRACT

Disinfecting powder food is challenging due to their low water activity. Intense-pulsed light (IPL) is advantageous in achieving efficient bacterial reduction. Its mechanisms of mediating bactericidal effect has been characterized as inducing DNA damage and disrupting cell structure integrity. A novel IPL platform is being constructed and studied to achieve high disinfecting efficacy while maintaining the physiochemical properties of the powder food. However, little is known about its influence on cell metabolism, which is essential for cell survival and growth. *E.coli* K-12 culture from overnight incubation were treated with a bactericidal dose of IPL for different durations. After centrifugation, the metabolites in bacterial pellets were extracted by a mixture of chloroform, methanol, and water. Aqueous and lipid extracts were examined by liquid chromatography-mass spectrometry (LC-MS)-based metabolomic analysis. The principal components analysis (PCA) of LC-MS data indicated that the metabolome of *E. coli* was dramatically affected by IPL treatment in a time-dependent pattern. Multiple nucleotides, antioxidants, and membrane components, including adenosine monophosphate, glutathione, and menaquinone-8, were identified as the metabolites sensitive to IPL treatment. These markers revealed IPL-induced membrane damage and oxidative stress. Additional markers suggest IPL hindered ability of repairing DNA damage. New information from untargeted metabolomic analysis provides useful insights on the mechanism of IPL-elicited bactericidal activities.

An ideal IPL treatment is expected to achieve pasteurization with minimal influences on physical, chemical, and nutritional properties of powdered food. While IPL showed effective bactericidal effect, it is also essential to evaluate its influence on the food

matrix. IPL-irradiated non-fat dry milk was prepared by solvent extraction and acid hydrolysis, and then examined by liquid chromatography-mass spectrometry (LC-MS) analysis. Targeted and untargeted chemometric analysis were performed to determine the chemical compositions of prepared samples and the effects of IPL treatment. Targeted chemometric analysis indicated that IPL treatment in this study did not significantly affect the amino acid composition of non-fat dairy milk powder. However, the multivariate models constructed by untargeted chemometric analysis of extracted samples revealed the dose-dependent chemical changes after IPL treatment. IPL treatment directly degraded riboflavin, and led to formation of peptides as a result of photolysis of milk proteins. Untargeted chemometric analysis on the chemical effects of IPL treatment will provide useful information to guide the development of IPL disinfection technology.

TABLE OF CONTENTS

List of Tables

List of Figures

Chapter 1 - Literature Review

Key words and abbreviations:

STEC, *Shigella* and *Shigella*-like toxin producing *Escherichia coli*; a_w, water activity; ESI electrospray ionization; FDA, Food and Drug Administration; NFDM, non-fat dry milk; PG, peptidoglycan; PE, phospshetidylethanolamine; LPS, lipopolysaccharide; TCA, tricarboxylic acid; ATP, adenosine triphosphate; USDA, United States Department of Agriculture; GC, gas chromatography; LC, liquid chromatography; NMR, nuclear magnetic resonance spectroscopy; MS, mass spectroscopy; FT-IR, Fourier transform infrared; TLC-FD, thin-layer chromatography with fluorescence detection ; LC-DAD, liquid chromatography with diode array detection; HCA, hierarchial cluster analysis; MLRC, multi-linear regression-calibration; PCA, principal component analysis; PLSl partial least square; PBS, phosphorus buffer solution; PLS-DA, projection to latent structures-discriminant; OPLS orthogonal partial least square; RT, retention time; *m/z*, mass to charge ratio; ROS, reactive oxygen species; NAD+, nicotinamide adenine dinucleotide.

1.1 Foodborne illness

1.1.1 Overview of foodborne illness

Foodborne illness is a persisting public health issue in the United States. From 2012 to 2016, over 800 cases of foodborne outbreaks were recorded each year, causing 103 deaths, more than 4000 hospitalizations, and over 71,000 illnesses [1]. *Escherichia coli*, *Listeria*, and *Salmonella* are the pathogenic bacteria responsible for most outbreaks through contaminating diverse food (Table 1.1), including ground beef, romaine lettuce, nuts, nut butter, flour, cheese, eggs, and sprouts [2]. Common complexions from

consuming contaminated food include abdominal cramps, diarrhea, nausea, fever, and vomiting. More severe consequences from food poisoning, such as *Clostridium botulinum* in canned foods, has caused respiratory failure and death [3]. Besides these adverse health effects, foodborne illness is also a significant economic burden for both public health agencies and individuals in the United States [4].

1.1.2 *Escherichia coli*

Escherichia coli is Gram-negative bacteria [5]. It is naturally distributed in the intestinal tract of warm-blooded organisms, including human [6]. Most strains of *E. coli* are non-pathogenic [7]. *E. coli* is intensively studied and widely used in a variety of research fields, such as genetic engineering, pharmaceuticals, molecular biology, and evolution [5]. *E. coli* K-12 is a non-pathogenic strain used widely in research as a surrogate [5]. Yet *E. coli* is well known to the public as a pathogen related to foodborne illness.

1.1.2.1 Pathogenic E. coli strains and foodborne illness

Even though majority of *E. coli* strains are nonpathogenic, a few *E. coli* strains can cause food poisoning, including *E. coli* O157:H7 and O26 [2]. Outbreaks are usually linked to fresh produces, ground beef, flour, and nuts (Table 1.1). Contamination are from environment and animals [8, 9]. From 1998 to 2006, more than 500 outbreaks were caused by pathogenic *E. coli*, which has led to more than 2,000 hospitalization and 38 deaths in the United States [1]. Symptoms of pathogenic *E. coli* infection include bloody diarrhea, abdominal cramp, and vomiting [3]. No specific treatment is targeting *E. coli* infection, except resting and adequate hydration aid in self recovery, according to Mayo Clinic [10]. However, severe form develops hemolytic uremic syndrome (HUS), most

commonly seen in immune compromised population and children under 5 years old. HUS is resulted from the shiga toxin and shiga-like toxin produced by *E. coli* O157:H7 and O26, also known as STEC [2, 3].These toxins act via binding to glycosphingolipid on the target cell surface, disrupting ribosomal RNA and sequential protein synthesis, and inducing apoptosis on renal tubular epithelial cells [11-13]. Severe HUS is characterized by degradation of red blood cells and renal kidney failure. Symptoms include fever, abdominal pain, pale skin tone, fatigue, and decreased urination. Testing of stool sample with microscopic visualization is a standard diagnostic procedure [14].

1.1.2.2 Overview of E. coli cell structure and metabolism

Both pathogenic and non-pathogenic *E. coli* strains share some essential cellular structure and metabolic features. The cellular structure of *E. coli* is shown in Figure 1.1 [15]. Prokaryotes like *E. coli* does not have bilayer-membrane organelles, such as mitochondria, and is much smaller in size than eukaryotes. *E. coli* is Gram-negative [5], with the cell wall consisting of an inner plasma membrane, a peptidoglycan (PG) cell wall, and an outer membrane. The plasma membrane consists by bilayer of predominantly phosphatidylethanolamine (PE), which accounts for 80% of total lipid [16]. Some proteins of important physiological functions are embedded in plasma membrane, including cytochromes, enzymes of electron transport chain, phospholipid synthesis enzymes, and active transporter proteins [17, 18]. PG cell wall consists of *N*-acetylmuramic acid and *N*-acetylglucosamine, joined by β-1, 4-glicosidic bond and cross-linked by oligopeptide bond. The outer membrane consists of one layer of lipopolysaccharide (LPS) and one layer of PE. LPS has the greatest susceptibility to oxidative damage, followed by phospholipid layers and then PG cell wall [15]. The

sandwich-style membrane structure is the target of some antibacterial agent and inactivation methods [19]. Disruption of the cell wall and membrane integrity alters the positive turgor pressure needed to maintain cellular structure competence and hence induce cell death [20]. *E. coli* cell has a flagella structure, which facilitates mobility and adherence to intestinal microvilli [21]. Its genetic material consists of genomic DNA, double-strand looped chromosomal DNA stored in nucleoid, with additional plasmid DNA, a circular double-strand DNA in cytoplasm separated from nucleoid. Chromosomal DNA contains genetic information that is essential for cellular function and growth. Plasmid DNA harbor genes that expresses antibiotic resistance and can replicate independently, which significantly aids in the survival of *E. coli* [22, 23]. Antimicrobial agents work in distinct mechanisms, but all involve disruption of bacterial DNA competence, stability, and replication. Nonetheless drug resistance still develops due to exchange of genetic material amongst bacteria cells [24].

Bacterial metabolism can be categorized into two categories: primary and secondary. Primary metabolites are essential for the normal function and growth of bacteria, including intermediates and end products of anabolic and catabolic pathways. Primary metabolites are also the foundation of synthesizing macromolecules and energy production. Examples include amino acids, nucleotides, vitamins, fatty acids, citric acid, acetate, and ethanol [25]. Secondary metabolites are not essential but might aid in cell survival. Shiga toxin and shiga-like toxin produced by *E. coli* O157:H7and O26 (STEC) are secondary metabolites. The central metabolism pathway of *E. coli* includes glycolysis, pentose phosphate pathways, and tricarboxylic acid (TCA) cycle, yielding adenosine monophosphate (ATP) and other important metabolites [26]. Glucose is the

primary carbon and energy source for *E. coli*. Lactose became the preferred fuel in glucose-poor environment [27].

Research has established several growth-limiting parameters for *E. coli* growth (Table 1.2). It is very flexible with the environment. *E. coli* can grow with temperature range from 7°C to 46°C, pH ranging from 3.56 to 9, and in NaCl up to concentration of 8.5% [28].

1.2 Disinfection technology and Intense Pulsed Light

1.2.1 Disinfection technology for different food matrix

Several disinfection technologies have been developed and approved to treat low-water activity foods.

Thermal treatment is a traditional disinfection technology. However, thermal treatment is not sufficient for disinfecting food of low water activity [29]. Bacteria, such as *Salmonella* spp. and *Cronobacter* spp. are highly resistant to heat in a low moisture environment, thus requires longer treatment with higher temperature to be completely inactivated [29]. However, undesired deterioration of food quality were reported to be associated with such thermal treatment, including production of volatile compounds [30], flavor [30], and color [31].

Non-thermal treatment have been studied for disinfecting dry foods. Application of chemicals, such as ethylene oxide and ozone, showed effective killing [32]. However, the use of ethylene oxide leaves residues in food and is banned in the European Union [33].

Ozone, on the other hand, does not leave residues, but alters food quality of those rich in unsaturated fatty acids and soluble proteins [34].

Ionizing irradiation technologies, such as electron beam, X-ray, and gamma ray, have been reported to be effective and are commercially adopted to disinfect dry herbs and spices in the U.S. [29]. Electron beam is environmental friendly, but has lower penetration and the disinfection effect is largely influenced by food size, thickness, direction, and package [35]. Gamma ray and X-ray had better penetration depth but the application of high dose irradiation adversely influences the food flavor [36]. Additionally, political factors and inadequate consumer advocacy limits the application and promotion of these irradiation technologies [37].

Use of ultraviolet (UV), a type of non-ionizing irradiation, is capable of deconstructing vegetative cells and spores and is commonly applied in pharmaceutical and medical products [38]. Due to its shallow penetration depth, in food system, continuous UV was studied for disinfecting juice, drinking water, and surfaces of fruits, vegetables, and fresh meat [38].Pulsed UV system was developed for disinfecting food powder. However, early alteration of food color was observed in flour and black pepper prior to reaching desired microbial log reduction [39].

Based on the characteristics and effectiveness of these technologies, they are applied to different food matrixes (Table 1.3), as approved by U.S. Food and Drug Administration (FDA). Most approved technologies are used in food surfaces and liquid food. Yet disinfecting powdered food remains a challenge, given the related outbreaks on flour,

milk powder, and chia seed powder [1]. Extensive research efforts are invested in developing feasible disinfection platforms for the food industry.

1.2.2 Challenges of disinfecting low-water activity powdered food

Powdered foods are unique of the low water activity (a_w) environment. This feature can be the result of processing, or the natural low moisture level [40, 41]. In general, low a_w food has an a_w <0.85, including milk powder, spices, powdered infant formula, flour, meal and grits, while the minimum a_w required for microbial growth is 0.6 [41]. Low a_w food are considered advantageous in terms of inhibiting the growth of pathogens in general [41]. However, some foodborne pathogens are able to survive in the dry environment, especially those who are in stationary phase or form spores [41]. During the drying process, the microbes do not grow, yet remain viable for extended period of time [42]. Once activated by moisture, survived pathogens can lead to diseases. Some bacterial strains can cause disease with only several living cells, such as some *Shigella* spp. Contaminated low-water activity food, such as nuts and dry milk, have become threat to public health and economic burden [40].

Powdered food is widely used as ingredients in food manufacturing and consumed directly [29]. Usually powdered food has low water activity (<0.85) [41]. Comparing to high-a_w food, which can be effectively pasteurized with mild heat treatment, low-a_w food is difficult to disinfect [41]. Insufficient disinfection of powdered food has led to outbreaks of foodborne illnesses over the years. Incidences were reported on dry milk powder[43], infant formula [44], powdered red and black pepper [45], and flour [46]. *Salmonella* spp. and *Cronobacter* spp. are two strains of bacteria associated with

foodborne illness incidences of dry milk products [29]. Other bacterial pathogens involved in outbreaks and recalls include *Bacillus cereus*, *Clostridium botulinum*, *Clostridium perfringens*, *Escherichia coli*, *Listeria monocytogenes*, and *Staphylococcus aureus*. The origin of these pathogens can be traced back to agricultural production, inadequate hygiene of the manufacturing environment and worker, and insufficient process control [29]. Industry have invested in reducing the risk of contamination from sources [41]. Yet, a dedicated and effective disinfection tool will be helpful for lowering the risk of foodborne illness and ensuring food safety [40].

1.2.3 Intense-pulsed light: mechanisms, advantages, and limitations

Intense-pulsed light (IPL) is an emerging non-thermal light-based disinfection technology [47]. The IPL emits broad spectrum light with wavelength range of 200-1100 nm, covering UV (200-400 nm), visible light (400-700 nm), and near-infrared (700-1100 nm) [48, 49]. Multiple flashes of light (1-20 per second) are delivered by the lamp containing energy up to 50 J/cm^2 at target surface. The intensity of the delivered light can be 20,000 times higher than sunshine [50] .FDA approved use of IPL in food processing in 1996.

Pulsed light technologies possess several advantages comparing to traditional (thermal) and other irradiation based technologies. Firstly, pulse light system deconstructs both vegetative cells and spores [47], which is effective for low water activity foods such as powdered food. Due to its nature of being a non-thermal technology, pulsed light is effective in decontaminating heat-resistant pathogens such as *Salmonella* spp.[50]. Meanwhile, IPL leaves no toxic or chemical residues to food matrix, which largely alleviates the concern on food safety. In addition, the IPL is more cost-efficient and

environmental friendly [51]. However, IPL has a shallow penetration depth (~2 mm), and is hence limited to applying for disinfecting food of low viscosity and high transparency, and food surfaces [47, 52]. Thermal effect of pulsed light technologies also raises concern for application on food with color, such as black pepper and flour. As a result of oxidative changes and heating, undesired color and flavor changes were observed prior to reaching ideal disinfection effect [39]. Hence, for commercial application, a good IPL system should have high penetration, thermal control, and well-validated process factors [53]. As the non-thermal IPL platform undergoes development, continuous monitoring on the processed food quality will be essential to evaluate the efficacy of the platform.

1.3 Non-fat dry milk

1.3.1 Production and pasteurization of non-fat dry milk

Non-fat dry milk is made from removing the moisture content of pasteurized fluid skim milk via spray drying process, without added vitamin A or D [54]. Fluid milk is pasteurized at specific temperature for designated amount of time prior to spray drying, according to USDA standard (Table 1.4) [54]. Current regulations do not require post spray dry disinfection. But the U.S. Standard Grade limits the bacterial estimate to no more than 75,000 CFU/gram as determined by standard plate count [55].

1.3.2 Nutrition profile of non-fat dry milk

Non-fat dry milk contains lipids, proteins, carbohydrates, proteins, vitamins, and minerals (Table 1.5). The lipid content is very minimal – 0.8g per 100g NFDM. Protein and carbohydrate are the major macronutrients, making up of about 35% and 55% of NFDM (Table 1.5). Bovine milk protein usually consists of 80% casein and 20% whey or serum

protein, which is made up by 7 major proteins: αs1-B casein, αs1-A casein, β-A2 casein, κ-B, α-lactoglobulin, β-lactoglobulin, and serum albumin [56, 57]. Milk proteins are complete proteins, and are primary source of essential amino acids for humans in milk [56, 58]. Milk contains many minerals. It is the primary dietary source of calcium in American's diet [58]. Phosphorus and potassium are also abundant in milk. As of vitamins, milk is good source of folate, vitamin A (retinoids), riboflavin, and vitamin B12 [58]. However, without fortification, vitamin A concentration is poor in NFDM and is not contributing to daily value (Table 1.5).

1.3.3 Quality parameters of non-fat dry milk

1.3.3.1. Color of milk

The color of milk is greatly attributed to the fat and micronutrient component. Skim milk contains less than 0.5% fat and skim milk powder contains no more than 1.5% fat [55, 59]. Skim milk appears more blue comparing to whole milk due to reflection of shorter wavelengths of visible light by casein micelles [60]. Micronutrients, riboflavin and β-carotene, contributes green and creamy color [61]. The white color is from proteins emulsified with casein micelle in milk fat globule membrane. USDA specifies U.S. grade non-fat dry milk to display "a uniform white to light cream natural color [55]."

Milk color can be measured in CIE Lab color space by use of a spectrocolourimeter, with color parameters indicating white (L^*), green (a^*) and blue (b^*) [62, 63]. Despite slight variation due to the source of milk, NFDM usually has L* value varying from 93.96 to 95.01, while the maximum of L* value is 100, indicating very white color [62]. The a^* value varies from -2.09 to -3.29, indicating a light green color detected in NFDM. With

b^* value ranging from 12.40 to 17.91, NFDM processes a color of yellowness. Total color difference is illustrated as ΔE^*, calculated as the square root of the sum of the squares of the different in each parameter, as shown in the following equation [64, 65]. It indicates the extent but not the direction of change [62]. Established system categorizes ΔE^*_{ab} values to three classes: not noticeable change ranging from 0 to 0.5; 0.5 to 1.5 means slightly noticeable change; over 1.5 indicates noticeable shift [64].

$$\Delta E* = \sqrt{\Delta L*^2 + \Delta a*^2 + \Delta b*^2}$$

Color is a quality parameter. Production season is an influential factor. Whole milk powder manufactured during summer shows lower L^* and higher b^* values due to the higher whey-protein level in raw milk [66]. Proper storage condition is crucial to maintain the quality, including color, of NFDM. Extended storage generates light brown color [67]. Extended processing during manufacturing exposes dry milk products to higher chance of color change. Color measurement is hence an essential parameter for quality monitoring of milk production. Different processing technologies influence milk color to various extents. Non-thermal processing methods, including pulsed electric field and microfiltration, showed less shift in total color space while exhibiting no significant difference in each parameter comparing to thermal pasteurized skim milk [63]. Pre-drying indirect heat treatment for 180 seconds at 90-93 °C resulted in significantly decreased L^* and higher b^* value in whole milk powder, which may be attributed by the browning product of Maillard reaction [60].

Change of the milk color is directly associated with chemical changes. Photo-degradation of riboflavin generates reactive oxygen species, which accelerates the decomposition of macro- and micro-nutrients [68, 69]. Milk is a rich source of riboflavin in American's diet. In fluid milk, sun light induced riboflavin photosensitization led to the degradation of tryptophan and tyrosine and resulted in brown color [69].

1.3.3.2. Protein

Milk protein has high biological value and is good source of essential amino acids [58]. The concentration of each major protein largely depends on the genetics, growth, and lactation status of the cow [56]. Exposure to light, UV or fluorescence, can lead to oxidative changes in milk protein structure and properties. Formation of carbonyl groups [47, 70-72], di-tyrosin [70, 71], and *N*-formylkynurenine [70, 71], and loss of tryptophan [71] were reported as indicators of protein oxidation. These markers are responsible for changes in primary, secondary, and tertiary structure of milk proteins [71]. Conformational changes of proteins were also reported as extensive proteolysis after exposure to UV, which eventually leads to reduced total bio-available protein content [70]. During the oxidative change process of milk proteins, riboflavin played a role as photosensitizer, aiding in the formation of singlet oxygen species [68] and accelerating the oxidative changes [71].

1.3.3.3. Carbohydrate

Lactose is the dominant carbohydrate present in milk, making up >50% of NFDM (Table 1.5). As a reducing sugar, lactose is capable of participating in the Maillard reaction: interacting with amino acids (mainly with lysine) at heated and non-heated condition [73,

74]. The joining of reducing sugar and lysine forms a Schiff base, which undergoes rearrangement and converts to Amadori product. After hydrolysis, furosine is formed [75]. Furosine (ε-N-2-furoylmethyl-L-lysine, FML) is usually used as an indicator of quality in many foods [73, 76]. Advanced Maillard reaction in milk leads to the color change (browning) [77], impaired availability of lysine [74] and digestibility of proteins [76].

1.3.3.4. Micronutrients

Milk significantly contributes to dietary riboflavin intake [78]. Riboflavin is resistant to heat processing but is sensitive to light [68]. In non-fat dry milk, photo-decomposition of riboflavin was reported to be a 2-phase process, with the 1st phase of fast and 2nd phase of slower degradation [79]. Both phases showed 1st-order reaction mechanism. Riboflavin can be oxidized to deuteroflavin and leucodeuteroflavin [68]. Generated riboflavin radicals have strong oxidative capacity and actively interact with amino acids, proteins, carbohydrates, and vitamins in food matrix, with and without oxygen present [68]. Tyrosine and tryptophan were reportedly sensitive to riboflavin radicals, degraded into dityrosin, indole-, flavin-, and indo-flavin-type aggregates. Histidine and methionine are also impacted. As of proteins, enzyme activity is reduced due to riboflavin induced photosensitization. Cross-link in collagen was also induced by riboflavin photosensitized modification [80]. Carbohydrate is more resistant to photo-oxidation, comparing to amino acids and lipids. Glucose can be degraded up to 30% with riboflavin at concentration of $10^{-6}M$ [81]. Multiple vitamins, including vitamin A, C, D, and E, can undergo degradation resulting from riboflavin-photosensitization. Vitamin A loss had the highest rate in non-fat milk [82]. Degradation product of vitamin A includes ethyl-(2,6,6-

trimethylcyclohex-1-ene) carboxylate, retinal, 5,8-peroxide of β-ionone, 5,6-peroxide of vitamin A, and retinoic acid [68]. Ascorbic acid is a strong antioxidant but is sensitive to photooxidation when oxygen and riboflavin are present [68]. Vitamin D is oxidized to 5,6-epoxide form, as a result of riboflavin's photo sensing and formation of singlet oxygen species.

Riboflavin's photosensitivity is directly associated with deterioration of milk flavor. Sulfur-containing compounds, methionine and dimethylsulfide are dominant contributor to the oxidized flavor in milk [68].

1.4 Technical platforms of metabolomics and chemometrics

1.4.1 Overview of metabolomics and chemometrics

Metabolomic platform has been an emerging technology for the past two decades. It refers to the study of the full profile of metabolites of a given subject. But the early concept of metabolomics, or metabolite profiling, can be traced back to the 1940s, when paper chromatography was used to identify and distinguish patterns amongst different subjects. It was believed that individuals processes unique metabolite pattern that can be identified in biological fluids [83]. With advances in technologies, including gas chromatography (GC), liquid chromatography (LC), and mass spectrometry (MS) through 1980s, and nuclear magnetic resonance spectroscopy (NMR) later, the application of metabolite profiling has been expanded in the field of system biology [84]. MS and NMR are the two analytical platform targeting small molecules. Comparing to NMR, MS has higher sensitivity and accuracy, and hence used more for metabolite detection, quantitation, and identification. Separating technologies such as LC and GC

are usually combined with MS. Additionally, combined with multivariate statistical analysis, the metabolomics have become a widely-used platform in areas including food, plant science, pharmaceuticals, toxicology, environmental science, and medicine [84].

Chemometrics, on the other hand, as a concept first brought up in 1970s [85]. It refers to application tools of chemistry with a combination of mathematical and statistical analysis, with an emphasis in the investigation of causal relationships [86]. Considering the nature of analytical chemistry of LC/GC-MS and NMR platform, and the use of multivariate data analysis, metabolomics can be considered as a chemometric approach, although chemometrics applies to a broader range of research. In addition to LC-MS platform, other analytical technologies are commonly used in chemometrics as well, including UV spectrometry, Fourier-transform infrared (FT-IR), raman spectroscopy, spectrofluorimetry, thin-layer chromatography with fluorescence detection (TLC-FD), and liquid chromatography with diode array detection (LC-DAD). Statistical tools commonly used in chemometrics include hierarchical cluster analysis (HCA), multi-linear regression-calibration (MLRC), principal component analysis (PCA), and partial least square (PLS) [87]. Chemometric based approach has now been widely used in fields of analytical chemistry [86].

1.4.2 Workflow of metabolomics and chemometrics

The workflow of metabolomics and chemometrics can be characterized into 4 steps: sample preparation, data acquisition, statistical modeling, and pathway analysis (Figure 1.1) [88].

Samples are prepared based on their biochemical and biological context. Appropriate sample preparation is essential for efficient and successful metabolomics study. The purpose of sample preparation is to remove unwanted particles and to extract metabolites and analytes from the sample matrix, and to make them applicable for the purpose of metabolomics analysis. In the context of cellular study, quenching cellular metabolism and extracting metabolites of interest is key to profiling the cell metabolome. Common method involves wash of phosphorus buffer solution (PBS), quenching with cold methanol, low-speed centrifugation, and a two-phase extraction by methanol-water-chloroform [89]. In the context of food, sample preparation involves more pre-treatment, such as grounding and freeze drying to enhance the efficacy of extraction [90]. The extraction method is largely similar to the ones for biological samples, based on extraction by methanol-water-chloroform. The two-phase extraction method maximize the release of compounds from sample matrix, and acquires both hydrophilic and hydrophobic analytes [90].

In addition to extraction, derivatization of chemicals with specific functional groups is commonly used prior to instrumental analysis, in order to enhance separation, selectivity and sensitivity. To detect organic acids, 2-hydraziniquinoline can be used as a derivatization agent.[91] It enhances the selectivity and detection of chemicals with carboxyl group [91]. Amino acid analysis is facilitated by derivatization with dansyl chloride [92].

Data acquisition in metabolomics is the key to high quality output. Three major platforms are currently used in metabolomics and chemometrics research: NMR, GC-MS, and LC-

MS, each with their own advantages and limitations [93]. NMR is based on the detection of emitted radio frequency in the strong magnetic field by nuclei between low and high energy spinstates [93]. It requires minimal sample preparation. In the context of cellular study, NMR can be used for metabolic profiling of intact cells and tissues [93, 94]. However, NMR has relatively low-sensitivity in comparison to LC-MS [95]. GC-MS is effective at separating and detecting volatile and small molecular weight compounds. But it is has very limited application for non-volatile and large compounds [96]. LC-MS is constructed based on separation of compounds in liquid chromatography, followed by electrospray ionization (ESI) and MS detection. It provides wider coverage and detection of metabolites with higher efficiency, and is able to provide structural analysis of unknown compounds [93]. But it requires sample preparation and derivatization, which can be time-consuming [95].

Obtained data usually went through extensive data mining and statistical analysis process. NMR spectroscopy yields spectrum (chemical shift and signal intensity). Subsequent data analysis involves assigning peaks to specific metabolites [93]. GC-MS and LC-MS yields retention time (*RT*) and mass to charge ration (*m/z*).[93] Annotating metabolites by *RT* and *m/z* is the basis of MS based data processing. Deployment of appropriate statistical analysis is essential to understand the highly abundant metabolomics data. Unsupervised approach, such as principal component analysis, can be used to classify samples, along with clustering analysis [88]. To characterize metabolites and biomarkers, projection to latent structures-discriminant analysis (PLS-DA) or orthogonal PLS (OPLS) can be used [97].

Metabolite identification is one of the foundations of data mining in metabolomics. Database in metabolomics analysis accelerates the workflow by providing automated annotation of spectra data, metabolite identification, and structural analysis [98]. Some commonly used mass spectrometry based metabolomics databases includes: Kyoto Encyclopedia of Genes and Genomes (KEGG, http://www.genome.jp/kegg), Human Metabolome Database (http://www.hmdb.ca), Lipid Maps (http://www.lipidmaps.org), METLIN database (http://metlin.scripps.edu), and MassBank (http://mona.fiehnlab.ucdavis.edu/). Development of algorithms and platforms also facilitates the data mining process by mapping out networks and pathways. Some analysis platform includes Metaboanalyst 4.0 (http://www.metaboanalyst.ca/MetaboAnalyst/faces/home.xhtml), MetaCore^{TM}, and 3Omics.

1.4.3 Application of chemometric analysis in food research

Chemometric applies to analysis of chemical based data, with data mining and statistical and mathematical methods. When it comes to food chemistry, traditional statistical methods focuses on analyzing the effect of one single variable at a time, which may be ignorant towards the nature complexity of food matrix. With the large amount of data generated by qualitative and quantitative food researches, the role of chemometric analysis has to investigate the interactions amongst sample matrix is becoming increasingly significant [99]. Combined with instrumental techniques, chemometric is

also part of data-mining tool of bioinformatics in foodomics, an emerging field in both food science and nutrition research.

Foodomics, a concept formed in the early 21st century, refers to the studies on food and nutrition using advanced -omics technology for the purpose of improving human nutrition [100, 101]. MS and NMR based technical platforms are essential to foodomic research. It is a combination of several disciplines: from traditional and advanced analytical chemistry technologies, to bioinformatics. Foodomics is applied to a variety of research areas, topics including food safety, food quality, prevention of food-related disease, authentication of genetically-modified food, and identifying and tracing contaminants [102].

Current -omics technology incorporated are genomic, transcriptomic, proteomic, and metabolomics. Metabolomics is the study of the full metabolome of sample species, focusing on the metabolites with mass smaller than 1000Da [101]. Separation technologies, such as LC, GC, and CE, are usually combined with MS in metabolomic studies, allowing for sensitive detection and measurement of low-abundance metabolites [90]. The metabolite changes associated with treatment can then be identified and used to establish patterns and causal relationships, which eventually form metabolic profiling and fingerprinting [88]. MS-based metabolomics approach has been successfully applied for studying food safety, quality, and traceability.

1.4.4 Application of metabolomics in microbial research

Metabolism is essential to all cellular functions [103]. Regulation and control over metabolism is fundamental for cell physiology and proliferation [103, 104]. Upon

environmental change, cells adopt a variety of mechanisms in different context to regulate metabolism in order to proliferate [103, 105]. The regulation occurs at genetic level, reflected by translation, transcriptional regulation of protein synthesis, and also post-translational modifications [104]. Disrupting the normal cellular metabolism can lead to cell death [106]. For example, in the context of bacterial cell, antibiotics bind to cellular targets and significantly impairs the availability of nicotinamide adenine dinucleotide (NAD^+), which further induce formation of reactive oxygen species (ROS), DNA damage, and eventually bacterial death [107].

The metabolites are embedded in the regulatory pathways, mediating and signaling the metabolic regulations and changes [105]. The concentration of metabolites directly reflect the microbial response to metabolic flux changes. Cell metabolomics studies and profiles these metabolites within living cells [108]. It provides a fast and effective method for screening a vast number of intracellular metabolites, and bridges genomics, transcriptomics, and proteomics [88, 109]. It provides a broader picture of system biology for cellular functions [109]. Cell and microbial metabolomics has a wide range of application in research [88, 105, 109]. In pharmaceutical field, cell metabolomics examines actions and targets of drugs [110, 111]. In cancer research, by characterizing cell metabolome, diseased cells can be differentiated from normal cells [103, 105], which facilitates the discovery of cancer biomarkers and disease diagnosis [112]. In microbial engineering, metabolomics revealed regulatory pathway and aid in the development of bacterial or yeast strains for bio-fuel production [113].

Table 1.1 Foodborne pathogens in the United States (Modified from Centers for Disease Control and Prevention List of Selected Multistate Foodborne Outbreak Investigations https://www.cdc.gov/foodsafety/outbreaks/multistate-outbreaks/outbreaks-list.html) [2]

Pathogen	Strain	Food contamination
Escherichia coli	O 157:H7	Romaine lettuce
		Leafy greens
		Nut butter
		Alfalfa sprouts
		Rotisserie chicken salad
		Ready-to-eat salads
		Ground beef
		Spinach and spring mix
		Hazelnuts
		Cheese
		Prepackaged cookie dough
		Pizza
		Beef patty
	O 121 and O26	Wheat Flour
		Raw clover sprouts
		Frozen food products
Listeria monocytogenes		Frozen vegetables
		Raw milk
		Packaged salads
		Soft cheese
		Ice cream
		Bean sprouts
		Cantaloupe

Salmonella	Braenderup	Shell eggs
		Nut butter
		Mango
	Typhimurium	Dried coconut
		Chicken salad
		Ground beef
		Cantaloupe
		Peanut butter
		Tomato
	Montevideo	Raw sprouts
		Pistachios
		Tahini sesame paste
	Newport	Cucumber
		Frozen shredded coconut
		Chia powder
		Cantaloupe

Table 1.2 Growth-limiting factors of *E. coli* [28]

	Minimum	Optimum	Maximum
Temperature (°C) *E. coli* (all types)	7-8	35-40	44-46
VTEC O157:H7 (Shiga-like toxin producing strain)	6.5	37	44-45
pH --Pathogenic *E. coli*	4.4*	-	9
water activity -- Pathogenic *E. coli*	0.95	-	-
Sodium chloride -- Pathogenic *E. coli*	Grows vigorously in 2.52% NaCl; Grow slowly in 6.5% NaCl; Does not grow in 8.5% NaCl		

**E. coli* O157 is reported to survive at pH values below 4.4 and has also been shown to grow at pH 3.6 in apple juice, pH 3.58 in hydrochloric acid, pH 3.78 in lactic acid and pH 3.96 in citric acid.

Table 1.3 Disinfection technologies and their application on different food matrix, approved by FDA

Disinfection technology	Examples of food matrix
Thermal	Liquid milk, meat products
Ozone	fish, poultry, fruits in storage, fresh vegetables, whole grains [114]
X-ray and gamma ray	Herbs, seeds, spices, poultry, meats, shell egg, shellfish [115]
UV	Fresh juice [115]

Table 1.4 USDA standard of pasteurization of fluid milk

Temperature	Time
145°F (vat pasteurization)	30 min
161°F (high temperature short time pasteurization)	15 s
191°F	1.0 s
194°F	0.5 s
201°F	0.1 s
204°F	0.05 s
212°F	0.01 s

Table 1.5 Nutritional profile of NFDM without added vitamin A (Modified from http://nutritiondata.self.com/facts/dairy-and-egg-products/83/2, based on USDA SR-21)

Macronutrients	Composition	Amount per 100g NFDM
Carbohydrate	Lactose	52.0 g
Protein	total	36.2 g
	tryptophan	510 mg
	threonine	1632 mg
	isoleucine	2188 mg
	leucine	3542 mg
	lysine	2868 mg
	methionine	907 mg
	cystine	334 mg
	phenylalanine	1746 mg
	tyrosine	1746 mg
	valine	2420 mg
	arginine	1309 mg
	histidine	981 mg
	alanine	1247 mg
	aspartic acid	2743 mg
	glutamic acid	7572 mg
	glycine	765 mg
	proline	3503 mg
	serine	1967 mg
fat	total	0.8g

Micronutrients	Composition	Amount per 100g NFDM
vitamins	vitamin A	7 mcg (22IU, 0%DV)
	vitamin C	6,8 mg (11%DV)
	vitamin D	332 IU (83% DV)
	vitamin K	0.1 mcg
	vitamin B1 (thiamin)	0.4 mg
	vitamin B2 (riboflavin)	1.5 mg
	vitamin B3 (niacin)	1.0 mg
	vitamin B6 (pyridoxine)	0.4 mg
	vitamin B12 (cobalamin)	4.0 mcg
	folate	50.0 mcg
	pantothenic acid	3.6 mg
	choline	169 mg
minerals	calcium	1257 mg
	iron	0.3 mg
	magnesium	110 mg
	phosphorus	968 mg
	potassium	1794 mg
	sodium	535 mg
	zinc	4.1 mg
	selenium	27.3 mcg

Figure 1.1 Workflow of Metabolomics and Chemometrics

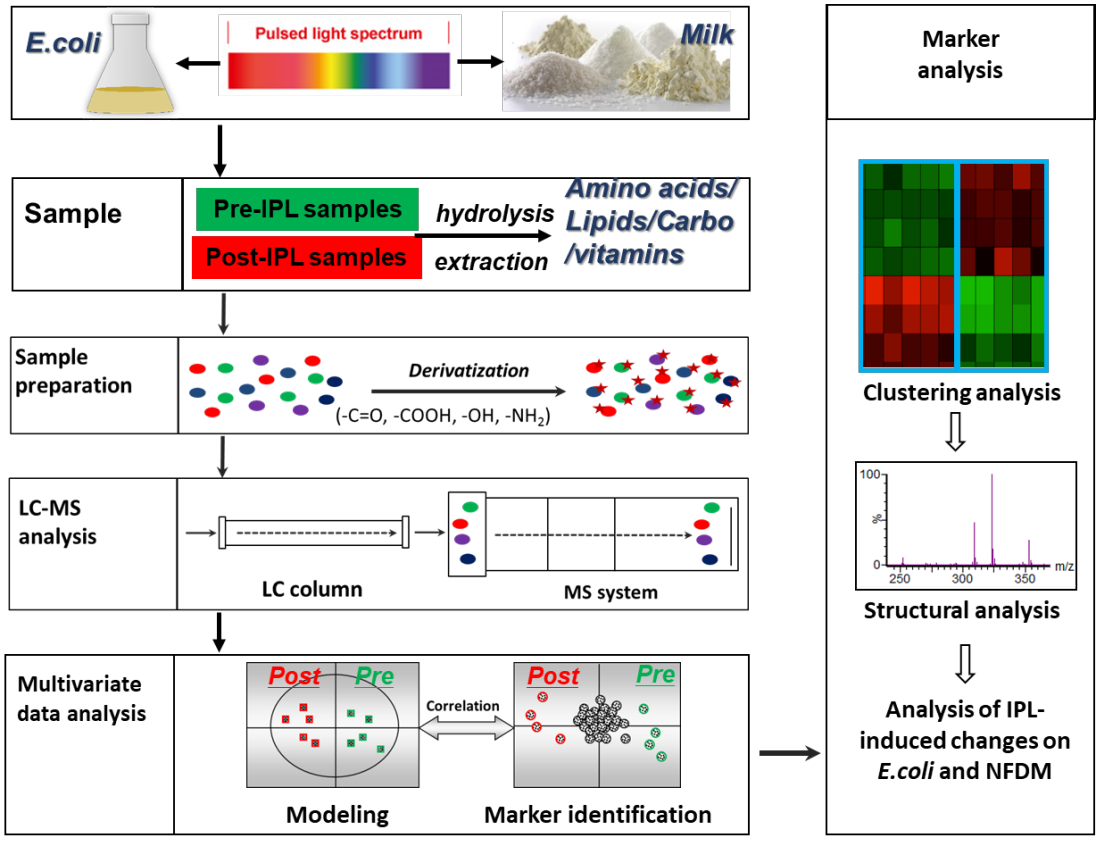

\

Chapter 2 - Metabolomics profiling intense pulsed light elicited bactericidal effect on *Escherichia. coli*

Key words and abbreviations:

STEC shiga and shiga-like toxin producing *E. coli*; HUS hemolytic uremic syndrome; UV-C untraviolet-C; a_w water activity; IPL intense pulsed light; ACN acetonitrile; DC dansyl chloride; LC-MS liquid chromatography-mass spectrometry; CMGSH 2-s-glytathionyl acetate; UMP uridine monophosphate; AMP adenosisne monophosphate; NAD^+ nicotinamide adenine dinucleotide; PCA principal component analylsis; HCA hierarchical cluster analysis; MK-8 menaquinone-8; UQH_2-8 ubiquinone-8; UQ-8 ubiquinone-8; PE phosphatidylethanolamine; GSH glutathione, reduced; GSSG glutathione, oxidized; MTA 5'-Deoxy-5'-(methylthio)adenosine; DHBA 2,3-dihydroxygenzoic acid; G3P glycerol 3-phosphate; GPDH glycerol-3-phosphate dehydrogenase; ROS reactive oxygen species; PBS phosphorus buffer solution; R5P ribose 5-phosphate; SEM scanning electron microscopy; TEM transmission electron microscopy

2.1 Introduction

Escherichia coli is a Gram-negative and facultative anaerobic bacterium that can live on diverse substrates in the intestinal tracts of animals and humans [8, 9]. *E. coli* is widely used as a model organism in microbiology research. Most of *E. coli* strains are non-pathogenic, but some shiga-toxin producing *E. coli* (STEC) strains, such as O157:H7 and O104:H4, are the causes of foodborne illnesses in the United States and Europe through contamination in vegetable, fruit, beverages, and undercooked meat [2]. General symptoms of STEC infection includes bloody diarrhea, vomiting, and abdominal pain. In

severe cases of infection, hemolytic uremic syndrome can occur, potentially leading to renal kidney failure and death [2, 3]. Therefore, effective disinfection of pathogenic *E. coli* is highly desirable in human food and animal feed production.

Thermal processing, which rises internal temperature of food to 70°C, is the most common technology to disinfect *E. coli* in food manufacturing [116]. However, thermal processing is known to alter physical and chemical properties of food. Other sterilization technologies, such as pulsed magnetic field [117], plasma under atmospheric pressure [118], high hydrostatic pressure [119], high pressure carbon dioxide [120], and ultraviolet-C (UV-C) irradiation [121], have been developed. Howbeit, these technologies have very limited application when applied to food matrix, especially dry foods of low water activity (a_w).

Intense pulsed light (IPL) is a novel non-thermal technology developed for inactivation of microbes in food of low water activity (a_w), such as powdered food. IPL system inactivates microbes by flashing (1-20 flashes per second) broad spectrum light (200-1100 nm) and delivering energy up to 50 J/m^2 to target surface [50].

The mechanism of IPL elicited bactericidal effect has not been fully explained. UV irradiation, making up of 25% of IPL, is an important component in IPL-induced bactericidal effect via photochemical changes [122]. Irreversible mutagenesis and DNA lesion are the dominant mechanism mediated by UV-induced cell death [123]. Studies have reported that there are differences between IPL and UV mediated cell damage. In addition to inducing DNA lesions, IPL disrupts cell structural and membrane integrity, leading to the leakage of intracellular content and eventually cell death. Moreover, IPL is

capable of denaturing protein, inactivating intracellular enzyme, and producing abnormal ion flow [124]. But the mechanism of the antimicrobial effect mediated by IPL needs further investigation.

Current understanding of pulsed light and UV elicited bactericidal effect is mainly based on targeted analysis, such as gel electrophoresis for analyzing DNA structural change[124, 125], scanning electron microscopy for cell histology[122], confocal laser scanning microscopy and flow cytometry for evaluating membrane damage [123, 125]. These analyses however reveal little information on cellular metabolic change, while maintaining normal metabolic activity is fundamental for cell proliferation [103, 104]. Metabolites, intermediates and end products of metabolic activities, directly reflects microbial response to environmental stress factors [108]. The metabolic activity changes induced by IPL remain unclear. Therefore, studying and analyzing the metabolites under IPL treatment can enhance the understanding of the mechanism of IPL-induced cellular metabolic changes.

Liquid chromatography-mass spectrometry (LC-MS) based metabolomics is a technical platform used widely in cellular and microbial research, such as cancer [112] and microbial engineering[113]. It is a high-throughput analytical platform, successfully profiles and fingerprints the changes in metabolome. It can be an efficient tool to further study the metabolic events occurred under IPL treatment in microorganisms.

In this study, the metabolic changes induced by IPL in *E. coli*, a representative foodborne pathogen, was studied by the LC-MS based metabolomics. The IPL-responsive metabolites were identified and characterized.

2.2 Materials and methods

2.2.1 Culture of *E. coli*

E. coli strain K-12 W3110 (ATCC 27325) was revived from frozen culture (-80°C) and maintained on TSA agar medium. Fresh inoculum was prepared by lifting a single bacterial colony from TSA agar medium and used to inoculate Luria-Bertani broth (EMD Millipore, Billerica, MA) and incubated at 37 °C for 12 h on a rotary shaker set to 200 rpm. Bacterial cells were harvested at an optical density (OD_{600}) of 1, transferred to 50 mL centrifuge tubes, and then centrifuged at 8000 rpm (Sorvall Legend XT/XF Centrifuge, ThermoFisher, Waltham, MA) for 10 min to pellet cellular suspension. After decanting the supernatant, the pellet was washed with phosphate buffered saline (PBS) (Millipore Sigma, Burlington, MA), and then re-suspended to the volume of bacterial culture.

2.2.2 IPL treatment of *E. coli*

The *E. coli* K-12 strain was chosen as the model of food-born pathogen to study the IPL-elicited bactericidal effects. In a separate study, the IPL instrument was designed and built to examine the efficiency of disinfection on bacteria inoculated food powder.

A 30 mL *E. coli* suspension in PBS was loaded in a petri dish (15 cm diameter) and then treated with IPL for 0 s (control), 5 s, 10 s, 15 s, and 20 s. Each second, 3 pulses of broad spectrum light (wavelength 190-1100 nm) with pulse width of 520 μs were elicited by a lab scale Z-1000 steripulse- XL system (Xenon Corporation, Woburn, MA, US), which consists of a xenon flash lamp and a RV-800 power control module. Each pulse delivers

1.27 J/cm at a distance from the lamp of 8 cm. Treated *E. coli* culture was chilled on ice for further analysis.

2.2.3 Chemicals

LC-MS-grade water and acetonitrile (ACN) were purchased from Fisher Scientific (Houston, TX). Dansyl chloride (DC), n-butanol, acetone, and amino acid standards were purchased from Sigma-Aldrich (St. Louis, MO).

2.2.4 Sample preparation for LC-MS analysis

IPL-treated and control *E. coli* culture was transferred to centrifuge tube and centrifuged at 5,000 × g 4 ºC for 10 min and washed with PBS twice. A 0.5 mL of methanol was added into the tube to re-suspend the pellet, then vortexed and sonicated for 30 s prior to transferring to 1.6 mL Eppendorf tube. Then 0.5 mL chloroform and 0.4 mL H_2O were added into the mixture and centrifuged at 14,000 × g 4 ºC for 10 min. Fractions were separated. Polar fraction was stored at -80 ºC, non-polar fraction was dried under nitrogen and reconstituted in 0.5 mL *n*-butanol.

2.2.5 Chemical derivatization

To detect amino acids, the polar fraction of *E. coli* extraction was derivatized with dansyl chloride (DC) prior to LC-MS analysis. Briefly, 5 µL sample or standard was mixed with 5 µL of 50 µM d5-tryptophan (internal standard), 50 µL of 10 mM sodium carbonate, and 100 µL of DC (3 mg/mL in acetone). The mixture was incubated at 60°C for 15 min and centrifuged at 14,000 × g for 10 min. Then supernatant was transferred to HPLC vial for LC-MS analysis.

2.2.6 Synthesis of standard

The standard of 2-S-glutathionyl acetate was synthesized based on previously established method [126]. Briefly, 100 µL of 100 µM glutathione was mixed with 100 µL of 10 mM iodoacetic acid in 10 mM ammonium bicarbonate buffer (pH=10, adjusted with ammonium hydroxide). The mixture was incubated at room temperature for 1h and then proceeded to LC-MS/MS analysis.

2.2.7 LC-MS analysis

A 5 µL aliquote of supernatant was injected into an Acquity ultra-performance liquid chromatography system (UPLC, Waters, Milford, MA). The polar fractions and derivatives were separated by a BEH C18 column or a BEH Amide column with a gradient of mobile phase ranging from water to 95% ACN containing 0.1% formic acid in a 10-minute run. The non-polar fractions were separated by a BEH C8 column with a gradient of mobile phase ranging from 55% A (60% H_2O, 40% ACN, 0.1% formic acid, 10mM NH_4OAc) to 100% B (methanol, 0.1% formic acid, 10mM NH_4OAc). The LC elute was directly introduced in a Waters QTOF mass spectrometer for accurate mass measurement and ion counting. For electrospray ionization, the capillary voltage was set at 3 kV and cone voltage was set at 40 V for positive mode detection. Nitrogen was used as both cone gas (50 liters/h) and desolvation gas (600 liters/h). For accurate mass measurement, the mass spectrometer was calibrated with sodium formate (range *m/z* 50-1,200) and monitored by intermittent injection of the lock mass leucine encephalin ($[M+H]^+$= *m/z* 556.2771) or reserpine($[M+H]^+$= *m/z* 609.2812) . Chromatograms were acquired and processed by MassLynx^{TM} (Waters). Structural of markers of interest was

analyzed by tandem MS (MS/MS) fragmentation with a collision energy ramp of 15-50 eV.

2.2.8 Multivariate data analysis

Chromatographic and spectral data were analyzed using MarkerLynx software (Waters). A multivariate data matrix containing information on sample identity, ion identity [retention time (RT) and *m/z*], and ion abundance was generated through centroiding, deisotoping, filtering, peak recognition, and integration. The intensity of each ion was calculated by normalizing the single ion counts (SIC) versus the total ion counts (TIC) in the whole chromatogram. The processed data matrix was further exported into SIMCA-P+^{TM} software (Umetrics, Kinnelon, NJ), transformed by Pareto scaling and then analyzed by principal components analysis (PCA). Major latent variables in the data matrix were described in a scores scatter plot of multivariate model. The potential chemical changes after IPL treatment was identified by analyzing ions contributing to the principal components and to the separation of sample groups in the loadings scatter plot. The chemicals' identity was identified by accurate mass measurement, elemental composition analysis, database search (Metlin, http://metlin.scripps.edu/; ECMDB, http://ecmdb.ca/), fragmentation, and comparison with authentic standards if possible.

2.2.9 Marker quantification

To quantify amino acids, the ratio between the peak area of each amino acid and the peak area of internal standard was calculated and fitted with a standard curve using QuanLynx^{TM} software (Waters).

2.2.10 Statistical analysis

Statistical analysis was performed by one-way ANOVA and Tukey – Kramer comparison test using the GraphPad Prism 6 (GraphPad Software, La Jolla, CA, US). $P<0.05$ is considered as statistically significant.

2.2.11 Transmission electron microscopy

IPL-irradiated *E. coli* was harvested by centrifuging at 5,000 × g 4 ºC for 10 min and washed with PBS twice. Cell pellet was processed by University of Minnesota Imaging Center (Saint Paul, Minnesota, United States) for transmission electron microscopy.

2.3 Results

2.3.1 IPL elicited log reduction of *E. coli*

Plate count of *E. coli* revealed significant log reduction after IPL treatment (Figure 2.1). Five log reduction was achieved after 10s, with further bactericidal effect alongside longer treatment time. The linear regression showed good correlation between the log reduction and IPL application, with the regression coefficient (r^2) of 0.81.

2.3.2 Modeling and identification of IPL induced changes in *E. coli* metabolome

E. coli K-12 culture was treated with IPL, from 0 to 20 s. Treated cells were extracted and separated to polar and organic phase, which were further analyzed by LC-MS. The features of LC-MS data were extracted and pooled together for PCA analysis. The distribution pattern of the PCA model of the *E. coli* metabolome showed that IPL treatment elicited progressive changes in the *E. coli* metabolome, mainly along the

principal component 1 of the model (Figure 2.2 A). All of the IPL-treated samples were distinctively different than the ones not treated by IPL (control samples). Moreover, the separation of IPL-treated samples illustrates a treatment-time dependent pattern. The metabolites contributing to the separation of control (0 s) and IPL treated samples were identified in a loadings plot (Figure 2.2 B and Table 2.1).

To examine the associations among the metabolites and IPL treatment, a hierarchical cluster analysis (HCA) based heatmap was constructed (Figure 2.3). Metabolite profile of IPL treated and control samples were dramatically different, indicating the significant effects of IPL on *E. coli* metabolome. Based on their metabolic function, and their origins in *E. coli* cellular structure, these metabolites were further characterized and categorized as the indicators of membrane component, amino acid metabolism, antioxidant metabolism, polyamine metabolism, and nucleotide metabolism.

2.3.2.1 Effects of IPL on E. coli membrane components

The loadings plot of the PCA model revealed three membrane lipid component were significantly reduced by IPL treatment: menaquinone-8, ubiquinol-8, and ubiquinone-8 (Figure 2.2 B). Menaquinone-8 (MK-8) was rapidly diminished upon 5 s of IPL treatment (Figure 2.4 A). Ubiquinol-8 (UQH_2-8) and ubiquinone-8 (UQ-8) were decreased dramatically after 5 s without further dose-dependent decrease (Figure 2.4 B and C). These trends were also observed in the LC-MS chromatogram. The LC-MS chromatogram of the organic phase showed UQH_2-8, UQ-8, and MK-8 eluting at 4.57, 5.11, and 5.83 min were diminished by IPL treatment after 20 s (Figure 2.4 D). The three major peaks eluted between 3 and 4 min were identified as membrane phospholipids:

PE(14:0/16:0) (*RT*=3.24), PE(16:0/19:1/9z) (*RT*=3.80), and PE(16:0/17:0CYCW7C) (*RT*=3.48). The intensity of the peaks of these three components remained unchanged after IPL treatment. However, since the overall features decreased, the relative abundance of these three lipids were reflected in the heatmap (Figure 2.3).

2.3.2.2 Effects of IPL on E. coli amino acid metabolism

The intracellular amino acids of *E. coli* culture were extracted in the polar phase and were detected by different LC-MS methods. Without derivatization, histidine was revealed as a major intracellular amino acid decreased by IPL treatment, as revealed by the chromatogram of the polar phase detected in negative ionization mode (Figure 2.5 G). With DC derivatization, the concentration of amino acids were more selectively quantified. IPL treatment decreased valine, glutamic acid, histidine, and pyroglutamic acid in *E. coli* (Figure 2.6 A-D). Glutamic acid was significantly diminished after 10 s of IPL treatment (Figure 2.6 B).

2.3.2.3 Effects of IPL on E. coli antioxidant metabolism

Glutathione, which is an antioxidant in functioning *E. coli* cells, was decreased progressively by IPL treatment (Figure 2.5 A). 2-S-glutathionyl acetate, also known as S-(carboxymethyl)glutathione (CMGSH), which is a derivative of glutathione (GSH), was absent in untreated cells and was increased progressively by IPL treatment (Figure 2.5 B). The changes of GSH and CMGSH were also reflected in the chromatogram in negative ionization mode. Eluting at 3.49 and 3.76 min respectively, GSH's concentration gradually declined while that of CMGSH was induced by IPL (Figure 2.5 G).

2.3.2.4 Effects of IPL on E. coli polyamine metabolism

Three *n*-acetylated polyamines were identified as IPL-responsive markers. *N*-acetylspermidine was increased by 5 s of IPL treatment and then decreased (Figure 2.7 A). *N*-acetylputrescine and *N*-acetylcadaverine decreased continuously with IPL treatment (Figure 2.6 E and F).

2.3.2.5 Effects of IPL on E. coli nucleotide metabolism

IPL increased two nucleotides level in *E. coli*: uridine monophosphate (UMP) and adenosine monophosphate (AMP) (Figure 2.5 B and C). The level of nicotinamide adenine dinucleotide (NAD^+) indicated a declining trend with progression of IPL treatment as shown in the LC-MS chromatogram (Figure 2.5 G). However, statistical analysis did not show significance (data not shown). Phosphoric acid, which is a common structural component in nucleotides, increased after IPL treatment (Figure 2.7 C). Additionally, 5'-Deoxy-5'-(methylthio)adenosine (MTA), a naturally occurring nucleoside, decreased with progression of IPL treatment (Figure 2.7 B).

2.3.2.6 Effects of IPL on other metabolites

IPL treatment increased 2, 3-dihydroxybenzoic acid (DHBA), an enterobactin breakdown product (Figure 2.7 D). Glycerol 3-phosphate (G3P), the backbone of glycerol phospholipids and ribose 5-phosphate (R5P), the intermediate and product of pentose phosphate pathway, were increased at 5s and then decreased with proceeded IPL treatment (Figure 2.5 E and F).

2.4 Discussion

Intense-pulsed light is a novel technology developed for disinfecting food of low water activity (a_w). Constituting of an important part of elicited light in the IPL system, UV irradiation is known to achieve bactericidal effect via DNA damage [123] and destruction of membrane integrity [124]. IPL also induces chromosomal DNA damage as a photothermal and photochemical effect. Additionally, IPL disrupts cellular integrity and structure [124]. However, the previous analysis was based on targeted analysis on DNA and structure integrity. As a hallmark of cellular function and activity, the effect of IPL on bacterial cellular metabolism is not fully studied. In this study, LC-MS based metabolomics analyzed the metabolome of *E. coli* affected by IPL, which may extend the understanding of the mechanism which IPL inactivates microorganisms.

2.4.1 IPL damages E. coli respiratory chain activity and disrupts membrane integrity

Menaquinone-8 (MK-8) and Ubiquinone-8 (UQ-8) are coenzymes specific to *E. coli* and located on the cytoplasmic membrane. They both consist of an aromatic ring and a polyprenyl hydrophobic tail [127]. They are best known as dominant components of membrane bound electron-transport chain. Besides, MK-8 and UQ-8 also play essential roles in anaerobic and aerobic respiratory growth, gene regulation, and oxidative stress management. MQ-8 also actively transport amino acids [128, 129]. Ubiquinol-8 (UQH_2-8) is reduced ubiquinone-8, functioning as scavenger of reactive oxygen species and hence has antioxidant property. The ratio of UQH_2/UQ indicates in vivo oxidative stress in animal cells [130]. However, the ratio of UQH_2/UQ did not experience significant change after multiple doses of IPL treatment (data not shown). Thus, the observed

decrease of UQ-8 and UQH_2-8 can be characterized as a direct effect elicited by IPL independent of potentially generated photo-oxidative stress. The level of UQ-8 and UQH_2-8 were reportedly reduced after continuous broad spectrum UVA irradiation in marine bacteria, with UQ-8 degraded earlier than UQH_2-8 [131]. However, upon IPL irradiation, both were degraded without significant further reduction by 5 s. (Figure 2.4 C and B), suggesting photosensitivity of UQ-8 and UQH_2-8. This is consistent with previously reported photosensitivity of quinones to near-UV light (300-380 nm) [132]. MK-8, also known as vitamin K2, shows exceedingly high photosensitivity to not only near-UV light (300-380 nm) but also visible light [129]. IPL contains near-UV and visible light, and hence led to acute photo degradation of MK-8 upon 5 s of IPL treatment. After 10s, MK-8 was depleted (Figure 2.4 A). Deficiency of functioning MK-8 hindered membrane transport of glutamic acid, as observed in *Bacillus licheniformis* [133], and delayed growth in *E. coli* [129]. Additionally, *E. coli* mutant depleted of MK-8 and UQ-8 could not grow in neither anaerobic nor aerobic conditions [134]. The IPL-elicited deleterious effect on MK-8 and UQ-8 is hence essential for inactivation of *E. coli* and preventing further growth of the remaining viable cells.

Glutamic acid, along with potassium, are the main cytoplasmic osmolytes for enteric bacteria, *E. coli* as an example [135]. Accumulation of potassium and glutamate is a protective strategy for coping with hyper-osmotic shock. Meanwhile, glutamic acid in the form of potassium salts provides stabilizing effect of DNA-protein interaction [136]. The concentration of glutamic acid in *E. coli* culture after IPL treatment did not experience any increase. Instead, upon 5 s, glutamic acid concentration was significantly lowered and was nearly depleted by 10 s (Figure 2.6 B). Such a dramatic change hence suggests

leakage of osmolytes as a result of IPL induced membrane damage, rather than a response to osmotic shock. Pyroglutamic acid is a common intracellular metabolite and is also a breakdown product of glutathione cycle [137]. *E. coli* incubated with hypochlorite experienced 2 fold increase of pyroglutamic acid as a result of oxidative stress [138]. However, the loss of pyroglutamic acid followed a treatment time dependent pattern, and is hence the result of cellular content leakage from permeable membrane. Additionally, the progressive loss of other intracellular amino acids (valine, histidine) (Figure 2.6 A and C), and *N*-acetylputrescine and *N*-acetylcadaverine (Figure 2.6 E and F) also indicate gradual alteration of membrane permeability after IPL treatment.

Intracellular content, such as amino acids and acetylated polyamines, carryout diverse and important metabolic functions bacteria such as *E. coli*. Loss of such content significantly hinders cell's normal physiological function and further growth. Leakage of intracellular content is a major contributor to IPL elicited inactivation of pathogens [47, 124].

Pulsed light is known to pose photothermal and photophysical effect to disrupt bacteria cell membrane integrity. Such effects result in cytoplasmic membrane shrinkage and cell wall destruction, which ultimately lead to cell death [47, 124]. Scanning electron microscopy (SEM) and transmission electron microscopy (TEM) examination of pulsed light treated cells clearly showed erupted cell walls, flattened and bursted cells [122-124]. The IPL treated *E. coli* cells will be examined by TEM, showing clear membrane and cellular structure. Ruptured cells are expected to be observed.

The photothermal effect is also suggested by the change of *N*-acetylspermidine. Acetylation of spermidine in *E. coli* was found as responsive to heat, cold shock, ethanol, and high pH [139]. Comparing to untreated controls, 5 s of IPL treatment induced increase of acetylated spermidine (Figure 2.7 A), indicating a potential heat shock due to the photothermal effect of IPL. But the proceeding loss of *N*-acetyspermidine might be the result of disrupted membrane permeability.

Glycerol 3-phosphate (G3P) is the backbone for synthesizing phospholipids in *E. coli* [140]. It can also be converted to dihydroxyacetone phosphate (DAP) by glycerol-3-phosphate dehydrogenase (GPDH) and then participate in gluconeogenesis pathways. GPDH is a cytoplasmic membrane bound respiratory chain enzyme, and is the key of glycerophosphate shuttle [141]. The acute rise of G3P upon 5 s of IPL might be the result of lowered activity of GPDH (Figure 2.5 E). Other respiratory chain component, such as MK-8, UQ-8, and UQH_2-8, were all significantly reduced upon IPL treatment. With increased IPL dose, G3P level progressively lowers, which could be the result of severe membrane damage and leakage of intracellular component (Figure 2.5 E). However, the stability of GPDH under photo irradiation warrants further study.

In human skin cells, the mitochondrial respiratory chain is considered to be the contributor of electron for forming reactive oxygen species (ROS) under UV irradiation [142]. Similar effect has been observed in *E. coli* under solar UV [143]. The respiratory chain enzymes, including NADH oxidase, succinate oxidase and lactate oxidase, lost their activity of energy metabolism upon small dose of UVA irradiation. The damage to these membrane bound enzymes further causes the cell to lose its membrane potential

and leads to membrane leakage [143]. In this study, the activity of these respiratory chain enzymes were not measured. But the dramatic loss of MK-8, UQ-8, and UQH_2-8, and the change of G3P level, all suggest that IPL hinders the normal metabolic activity of respiratory chain. While mainlining the metabolic activity of the respiratory chain is essential for cell viability and growth, therefore the IPL induced damage of respiratory chain and the following membrane damage is a key mechanism which ultimately mediates cell death.

2.4.2 IPL induces oxidative stress and changes in redox balance system

Having different cellular and metabolic functions, the level and changes of several metabolites indicates IPL had induced oxidative stress on *E. coli* cells.

The level of 2, 3-dihydroxybenzoic acid (DHBA) increased followed an IPL-dose dependent manner (Figure 2.7 D). DHBA is a natural occurring phenolic acid in *E. coli*, functioning as iron chelator and is a moiety of iron's siderophore, enterobactin [144]. Enterobactin has protective effect on *E. coli* upon oxidative stress, and is crucial for colony development [145]. DHBA also scavenges peroxyl radicals [144, 146]. Upon oxidative stress of hydrogen peroxide in growth media, the production of DHBA significantly increased in *E. coli* [144]. Upon 5 s of IPL treatment, DHBA's level increased significantly and continued to increase with proceeding IPL doses, indicating the continuous breakdown of enterobactin. This is also a sign of oxidative stress directly induced by IPL.

Glutathione (GSH), a well-established antioxidant in glutathione-ascorbate cycle of functioning cells, experienced gradual loss upon IPL treatment. To maintain redox

balance, GSH is oxidized to oxidized glutathione (GSSG). However, in IPL treated cells, the level of GSSG did not show significant variance across treatment groups (data not shown). Therefore, the gradual reduction of GSH level was not associated with IPL induced oxidative stress. However, 2-s-glutathionyl acetate (CMGSH), a glutathione derivative (by blockage of thio group) was formed after IPL treatment. CMGSH is best known as an intermediate during the metabolism process of xenobiotics like 1,1-dichloreothylene by cytochrome P450 [147]. The association between light irradiation and the formation of CMGSH has not been reported before. In most cases, CMGSH is formed by incubating GSH with iodoacetate or chloroacetate, as a strategy to detect and quantify GSH [148]. But the *E. coli* was suspended in phosphorus buffer solution (PBS) where either iodoacetate or chloroacetate was absent. Yet the formation of CMGSH is a dominant feature in *E. coli* metabolome after IPL treatment, as observed in the LC-MS chromatogram (Figure 2.5 G). Hence, the loss of GSH and formation of CMGSH appears to be mediated by IPL irradiation. With the thiol group blocked, GSH cannot be transformed to GSSG and hence loses its antioxidant property, which may hinder further cell viability. It hence can be used as a marker to determine cell culture viability. However, the mechanism of pulsed light irradiation induced formation of CMGSH warrants further investigation.

Ribose 5-phosphate (R5P) is a product formed from pentose phosphate pathway, used for synthesis of nucleotides and nucleic acids. The production of R5P also couples the synthesis of NADPH, a reducing equivalent participating in reductive biosynthesis pathways [149]. In human skin cells, activation of pentose phosphate pathway was characterized as a first response to UV oxidative stress, marked by increased production

of R5P [150]. With the boost of R5P at the first 5 s of IPL, it can be speculated that *E. coli* responded to IPL induced oxidative stress in the first 5 s in a similar pattern observed in human skin cells. But the following dramatic decline suggests a potential leakage as a result of permeable membrane (Figure 2.5 F).

2.4.3 Effect of IPL on DNA damage and repair

Adenosine monophosphate (AMP) and phosphoric acid are structural moieties of adenosine triphosphate (ATP). The IPL-dependent increase of AMP and phosphoric acid level suggests a gradual breakdown of ATP (Figure 2.5 D, Figure 2.7 C)). Meanwhile, previous study has reported impaired ATP synthesis in *E. coli* after UVA irradiation [143]. ATP is one of the fundamental intracellular energy carriers, participating in many metabolic process, such as protein synthesis. ATP is also needed for DNA replication, repair, and RNA synthesis [151-153]. Cell under stress needs ATP as the readily available energy for defending and surviving stress [143]. Previous study revealed that IPL is capable of inducing DNA damage in pattern similar to UV irradiation [123]. IPL induced hydrolysis of ATP potentially will further makes it more difficult for remaining viable *E. coli* cells to repair DNA damages in the dark cycle.

Uridine monophosphate (UMP) is the building block of RNA. The accumulation of UMP in IPL-treated cells (Figure 2.5 C) potentially suggests the blockage of RNA synthesis pathways. RNA synthesis is essential for protein synthesis and plays a central role in cellular function. The blockage of such pathway ultimately hinders *E. coli*'s metabolic activity and leads to cell death.

2.4.4 Summary of IPL treatment time dependent modification on E. coli metabolome and cellular physiology

The multi target inactivation mediated by IPL treatment on *E. coli* follows a treatment-time-dependent pattern.

In the first 5 s, large amount of cells still remain viable. The increase of *N*-acetylspermidine and R5P suggests the *E. coli* initiated defensing system in response to IPL-induced oxidative stress. However, with further degradation of membrane bound respiratory chain components , evidenced by the change of MK-8, UQ-8, UQH_2-8, and other intracellular metabolites, the resistance to oxidative stress was diminished. The alternation of membrane integrity and permeability ultimately lead to cell death in *E. coli*.

2.4.5 Implication on development of IPL instrument

To investigate the bactericidal effect elicited by IPL, *E. coli* was cultured, treated by IPL, and then the metabolome examined. LC-MS based metabolomics analysis revealed that IPL induced *E. coli* cell death by damaging membranes, disrupting cellular structure integrity, and posing oxidative stress. Studying the mechanism of IPL-elicited effect on *E. coli* provides innovations for the future development of IPL platform. Several photo-sensitive components in *E. coli* was identified to be contributing to cell death, suggesting potential enhancement of corresponding light source for greater bactericidal effect in future IPL models. In addition, *E. coli* can be seen as a Gram-negative bacteria model. Foodborne illnesses can be caused by other microorganisms, including Gram-positive and spore forming bacteria. Comparing to Gram-negative bacteria like *E. coli*, Gram-

positive bacteria do not have the outer membrane [5]. Spores, on the other hand, do not have cellular structure – mostly consisting of a protein-rich inner and outer coats, cortex, and core of DNA [154]. *Bacillus cereus* is an example of Gram-positive and spore forming bacteria that causes foodborne illness [29]. It is highly resistant to heat, cold, dryness, and radiation [155]. In a separate research project, IPL is developed to inactivate spores in low a_w powder food. Potential studies on spores and Gram-positive species can be performed to evaluate and to compare the IPL-elicited effects. The common features elicited by IPL on these species could probably be revealed by LC-MS based metabolomics, which could be emphasized in future IPL models to improve the pasteurization capability.

Table 2.1 IPL-responsive metabolites in *E. coli* metabolome revealed by the loadings plot of the PCA model

Detection phase	Metabolites decreased by IPL	Metabolites increased by 5s IPL	Metabolites increased by 20s IPL
Organic	ubiquinol-8, menaquinone-8, ubiquinone-8,	N/A	N/A
Polar	pyroglutamic acid[a], valine[a], glutamic acid[a], histidine[a], 5'-deoxy-5'-(methylthio)adenosine[a], glutathione[a]	glycerol 3-phosphate[a], ribose 5-phosphate, *N*-acetylspermidine	uridine monophosphate (UMP)[a], adenosine monophosphate(AMP)[a], 2-s-glytathionyl acetate (CMGSH)[a], 2,3-dihydroxybenzoic acid (DHBA), phosphoric acid[a]
Polar, DC derivatized	pyroglutamic acid, *N*-acetylputrescine[a], *N*-acetylcadaverine, glutamic acid[a]	N/A	N/A

[a]The structural identities of these metabolites were determined by comparing with authentic standards. Other metabolites were elucidated by MSMS fragmentation.

Figure 2.1 Plate count of *E. coli* after IPL treatment. A linear regression model was created, with the f^2 as 0.81.

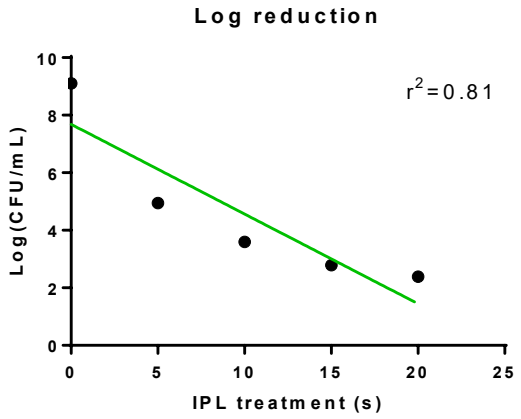

Figure 2.2 Principal component analysis of *E. coli* metabolome. A: Scores plot of PCA model. Untreated and IPL-treated samples were separated mainly on the direction on the first component. B: Loadings plot of PCA model. Markers high in untreated control and IPL treated samples were identified.

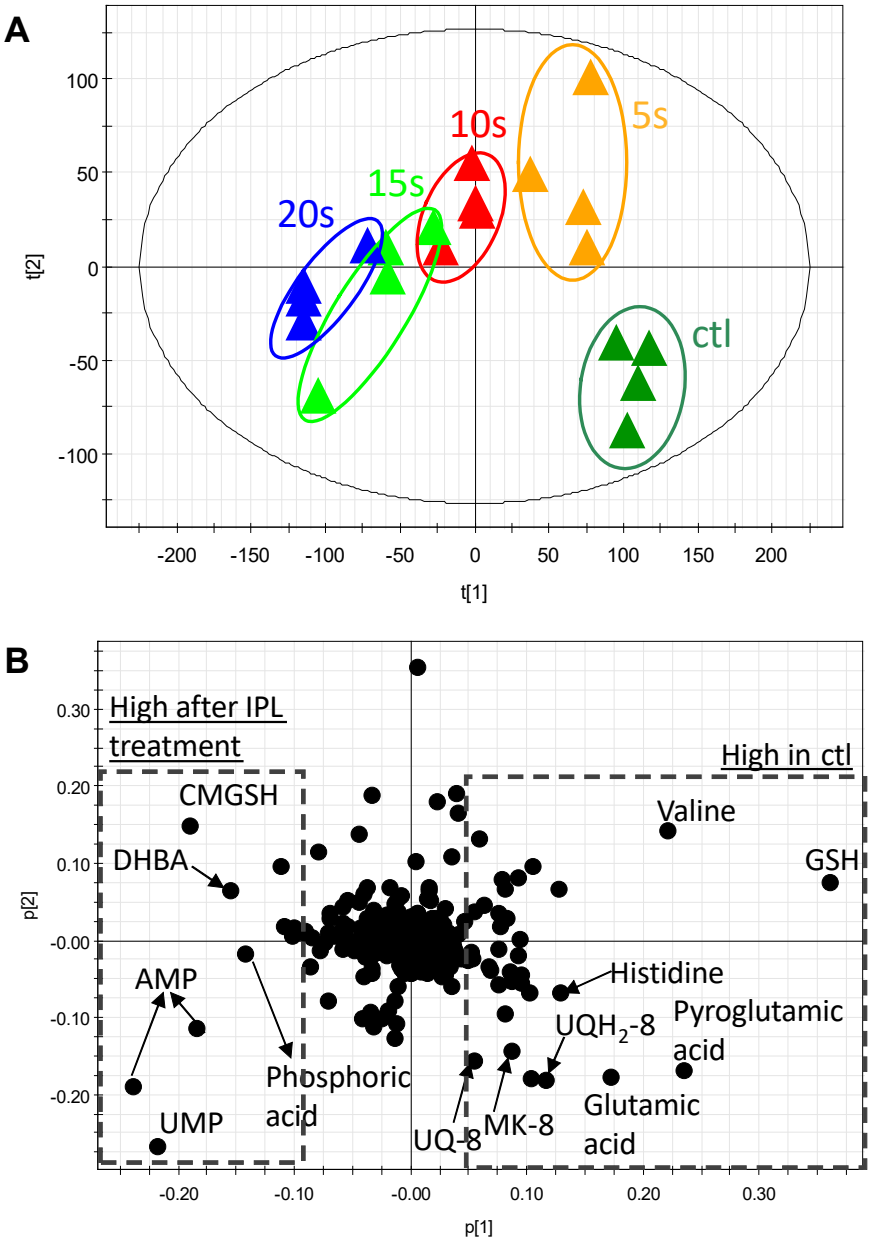

Figure 2.3 Heatmap of IPL-responsive markers.

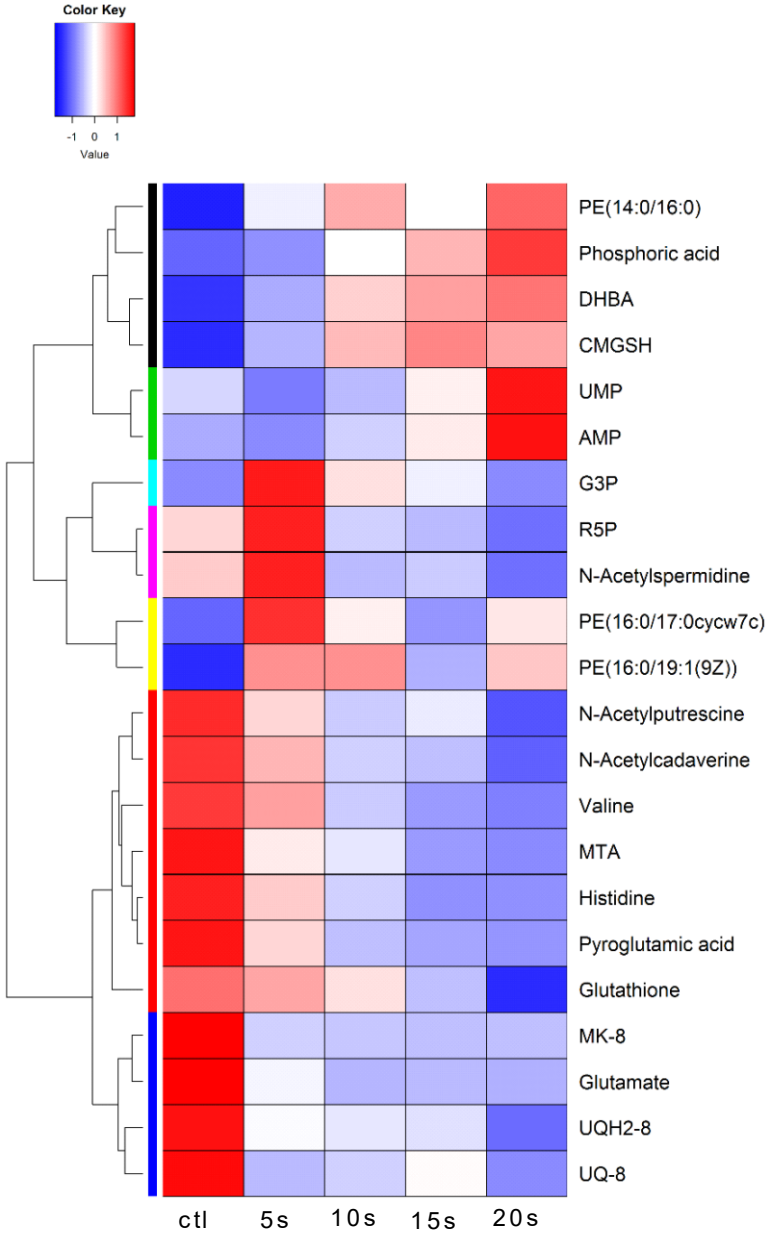

Figure 2.4 IPL-responsive membrane components of *E. coli* revealed by loadings plot of PCA model. (A) Menaquinone-8 relative abundance. (B) Ubiquinol-8 relative abundance. (C) Ubiquinone-8 relative abundance. (D) Chromatogram of the organic phase of *E. coli* metabolome. Ubiquinol-8 (RT= 4.57), ubiquinone-8 (RT=5.11), and menaquinone-8 (RT=5.83) were the three compounds diminished by 20s of IPL treatment.

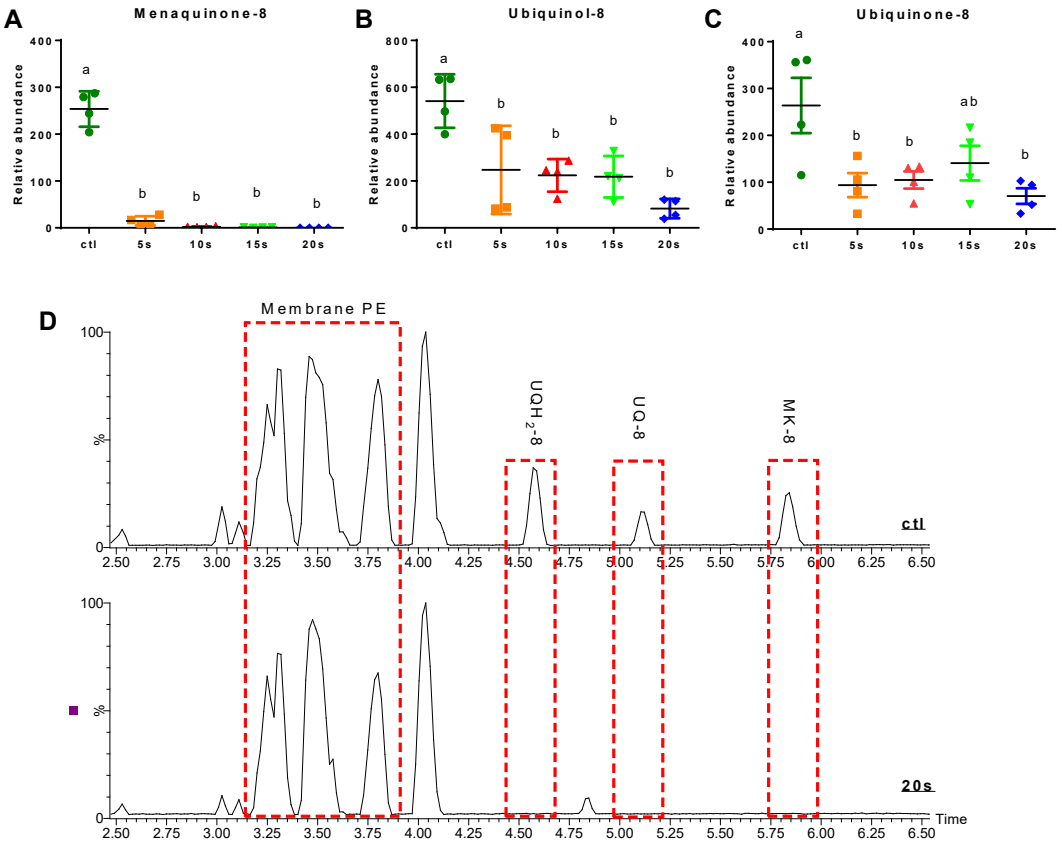

Figure 2.5 IPL-responsive markers detected in polar phase extraction of *E. coli* in negative ionization mode by LC-MS. (A) Relative abundance of glutathione. (B) Relative abundance of 2-s-glutathionyl acetate. (C) Relative abundance of uridine monophosphate. (D) Relative abundance of adenine monophosphate. (E) Relative abundance of glycerol 3-phosphate. (F) Relative abundance of ribose 5-phosphate. (G) Overlay of LC-MS chromatograms.

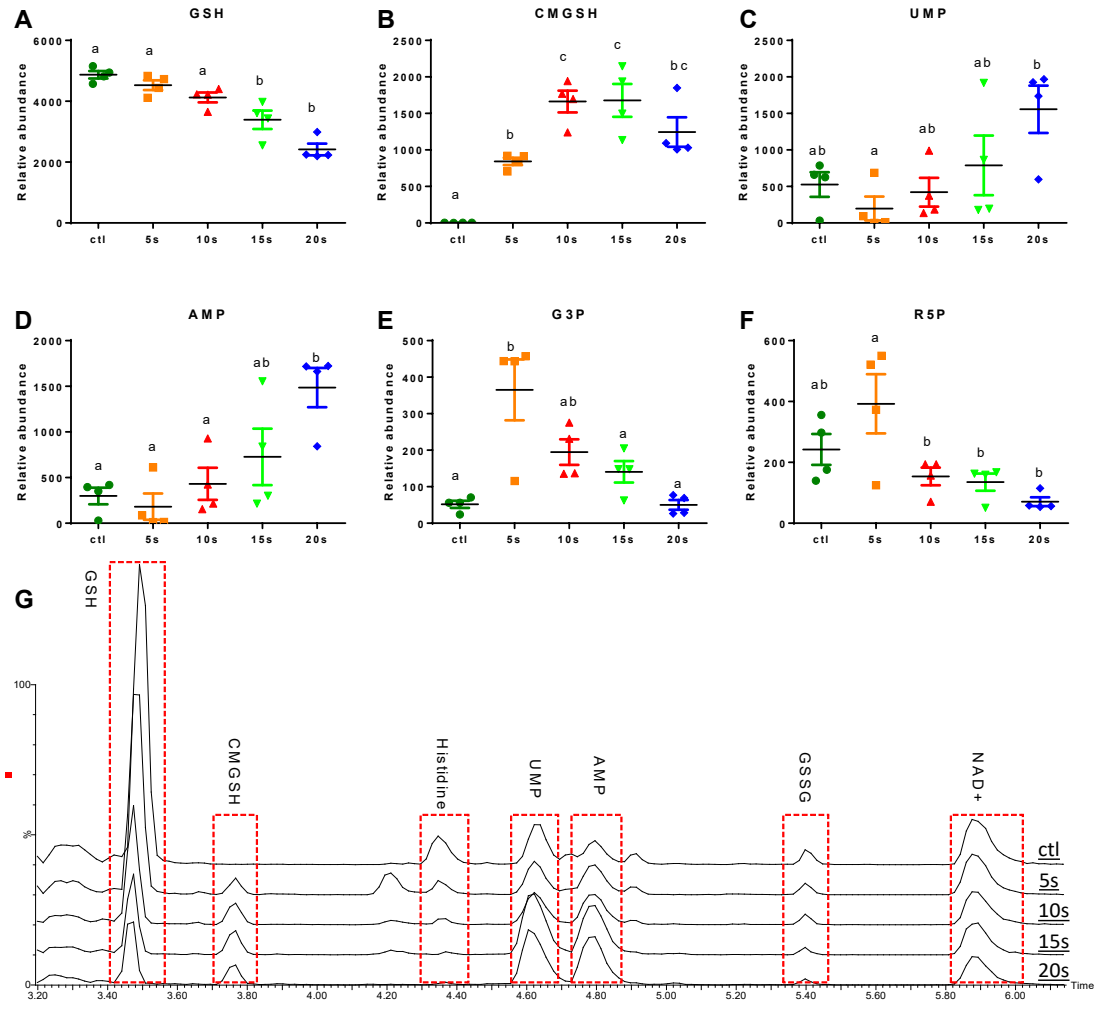

Figure 2.6 IPL-responsive metabolites detected with dansyl chloride (DC) derivatization. Amino acids were quantified with authentic amino acid standards and the concentration was shown as μM. (A) Concentration of valine. (B) Concentration of glutamic acid. (C) Concentration of histidine. (D) Relative abundance of pyroglutamic acid. (E) Relative abundance of *N*-acetylputrescine. (F) Relative abundance of *N*-acetylcadaverine.

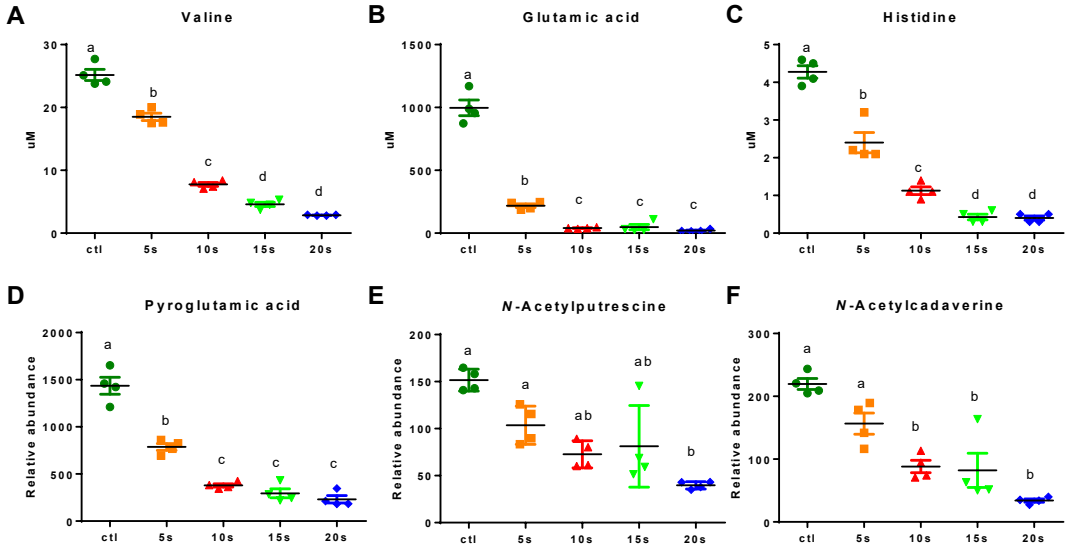

Figure 2.7 IPL responsive markers in polar phase extraction of *E. coli*, detected in positive ionization mode without derivatization. Relative abundance of (A) *N*-acetylspermidine, (B) 5'-deoxy-5'-(methylthio)adenosine, (C) phosphoric acid, (D) 2, 3-dihydroxybenzoic acid

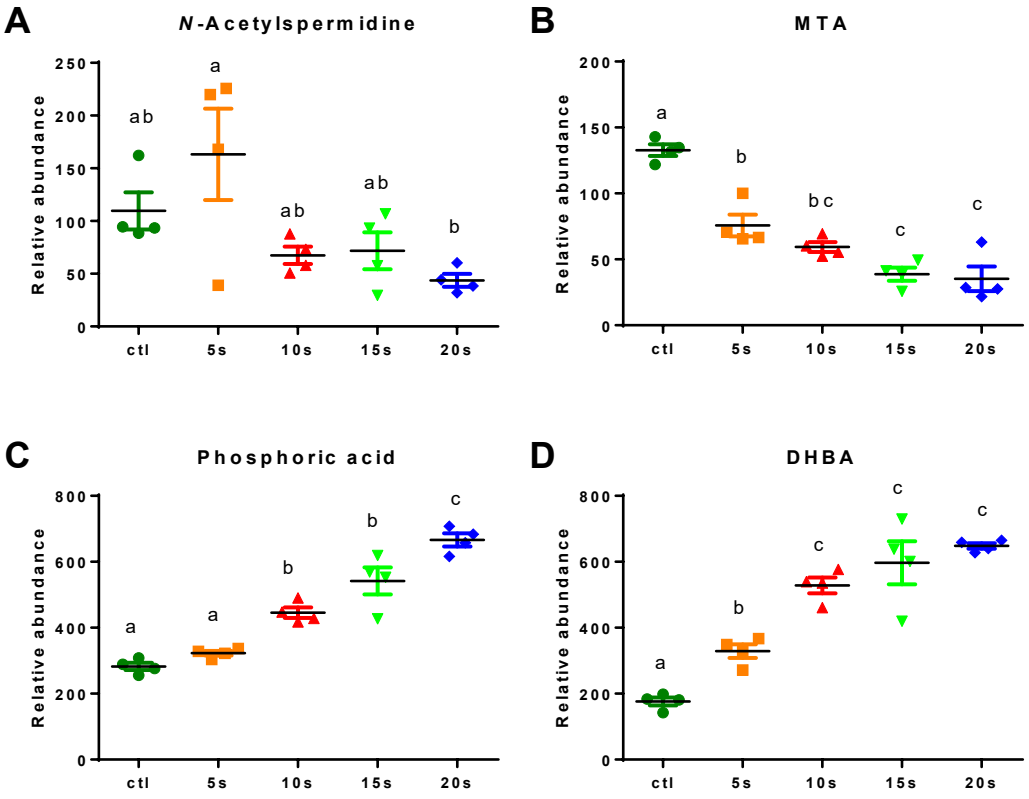

Chapter 3 - Profiling intense pulsed light elicited effect on non-fat dry milk by LC-MS based chemometrics

3.1 Introduction

Non-fat dry milk is a low water activity powdered food, used widely in production of processed foods, such as in bread, canned soup, animal food, and infant formula [156]. It is manufactured from spray drying of pasteurized skim milk [54]. The characteristic of low water activity food makes it challenging to ensure the complete safety of NFDM. Although USDA posts regulation with total bacteria count in spray dried NFDM [55], there is not yet a dedicated procedure for disinfecting NFDM. *Cronobacter* spp. (formerly *Enterobacter sakazakii*) is a Gram-negative bacteria associated with foodborne illness of dry foods, including dry milk and infant formula. It causes meningitis, necrotizing enterocolitis and sepsis in infants [156].

Intense pulsed light has shown to be effective at disinfecting food surfaces and liquid food [47, 52]. It is potential to be applied to powdered food disinfection. In a separate study, the efficacy and efficiency of bactericidal effect of IPL platform is evaluated. However, previous studies have reported deterioration of food quality prior to reaching desired disinfection effect. For example, apples appeared more browning after pulsed light treatment due to destruction of pectin cell wall [157]. Flour and black pepper experienced significant color shift prior to completing pasteurization [39].

In this study, the effect of IPL on non-fat dry milk's chemical profile was investigated by LC-MS based chemometric analysis. The chemical markers associated with dose-dependent effect of IPL were identified and characterized.

3.2 Materials and method

3.2.1 IPL treatment of non-fat dry milk

Non-fat dry milk without fortification (Land O'Lakes) was chosen as the model of powdered food to study the IPL-elicited effects. In a separate study, the IPL instrument was designed and built to examine the efficiency of disinfection on bacteria inoculated food powder. NFDM without bacteria inoculation was processed by the IPL instrument. Briefly, NFDM was loaded into a vibratory treatment chamber, then treated by IPL for 1-4 passes with each pass equivalent to 28 s. Each second, 3 pulses of broad spectrum light (wavelength 190-1100 nm) with pulse width of 520 us were elicited by a lab scale Z-1000 steripulse- XL system (Xenon Corporation, Woburn, MA, US), which consists of a xenon flash lamp and a RV-800 power control module. Each pulse delivers 1.27 J/cm^2 at a distance from the lamp of 8 cm. Treated NFDM was collected and store in air-tight centrifuge tubes at -20 °C.

3.2.2 Color measurement of non-fat dry milk

Color of NFDM was measured by a colorimeter (Konica Minolta CR-300 Chroma Meter). Briefly, NFDM was placed in a petri dish (60 x 15 mm) and pressed down. Then the color was measured and recorded as CIE *L*a*b** color space.

3.2.3 Chemicals

LC-MS-grade water and acetonitrile (ACN) were purchased from Fisher Scientific (Houston, TX). 2-Hydrazinoquinoline (HQ) and triphenylphosphine (TPP) were purchased from Alfa Aesar (Ward Hill, MA). 2-2'-Dipyridyl disulfide (DPDS) were purchased from MP Biomedicals (Santa Ana, CA). Dansyl chloride (DC), *n*-butanol,

acetone, and amino acid standards were purchased from Sigma-Aldrich (St. Louis, MO). Hydrochloric acid was purchased from Honeywell (Morristown, NJ).

3.2.4 Sample preparation for LC-MS analysis

To determine the influence of IPL on NFDM's amino acid composition, 50 mg of non-fat dry milk was dissolved in 7 mL 6N hydrochloric acid for acid hydrolysis. Acid hydrolysis was performed at 165 °C for 15 min by a Discover SP-D microwave digester (CEM Corporation, Matthews, NC). After hydrolysis, 50 µL of hydrolyte was dried by nitrogen and then reconstituted in 500 µL 50% aqueous ACN.

Extraction of NFDM was based on the principal of two phase (methanol-water-chloroform) extraction that is commonly used in preparing food samples for chemometric analysis [90]. Briefly, 50 mg of NFDM was dissolved in 0.5 mL methanol, 0.5 mL chloroform and 0.4 mL water. After 10 min centrifuge at 14,000 × g, fractions were separated. Polar fraction was stored at -80 °C; non-polar fraction was dried under nitrogen and reconstituted in 0.5 mL *n*-butanol.

3.2.5 Chemical derivatization

To detect amino acids, the hydrolyte was derivatized with DC prior to LC-MS analysis. Briefly, 5 µL sample or standard was mixed with 5 µL of 50 uM D5-tryptophan (internal standard), 50 µL of 10 mM sodium carbonate, and 100 µL of DC (3mg/mL in acetone). The mixture was incubated at 60°C for 15 min and centrifuged at 14,000 × g for 10 min. Then supernatant was transferred to HPLC vial for LC-MS analysis.

To detect carboxylic acids, aldehydes, and ketones, the polar fraction of NFDM extraction was derivatized with HQ prior to LC-MS analysis. Briefly, 2 µL of the sample

was added into a 100 µL freshly-prepared ACN solution containing 10 mM DPDS, 10 mM TPP and 10 mM HQ. The mixture was incubated at 60 °C for 30 min and then immediately chilled on ice, followed by an addition of 100 µL of H_2O. After centrifugation at 14,000 × g for 10 min, the supernatant was transferred to HPLC vial for LC-MS analysis.

3.2.6 LC-MS analysis

A 5 µL aliquote of supernatant was injected into an Acquity ultra-performance liquid chromatography system (UPLC, Waters, Milford, MA) and separated in a BEH C18 column or a BEH Amide column with a gradient of mobile phase ranging from water to 95% ACN containing 0.1% formic acid in a 10-minute run. The LC elute was directly introduced in a Waters QTOF mass spectrometer for accurate mass measurement and ion counting. For electrospray ionization, the capillary voltage was set at 3 kV and cone voltage was set at 40 V for positive mode detection. Nitrogen was used as both cone gas (50 liters/h) and desolvation gas (600 liters/h). For accurate mass measurement, the mass spectrometer was calibrated with sodium formate (range *m/z* 50-1,200) and monitored by intermittent injection of the lock mass leucine encephalin ($[M+H]^+$= *m/z* 556.2771). Chromatograms were acquired and processed by MassLynx^{TM} (Waters). Structural of markers of interest was analyzed by tandem MS (MS/MS) fragmentation with a collision energy ramp of 15-50 eV.

3.2.7 Multivariate data analysis

Chromatographic and spectral data were analyzed using MarkerLynx software (Waters). A multivariate data matrix containing information on sample identity, ion identity

[retention time (RT) and *m/z*], and ion abundance was generated through centroiding, deisotoping, filtering, peak recognition, and integration. The intensity of each ion was calculated by normalizing the single ion counts (SIC) versus the total ion counts (TIC) in the whole chromatogram. The processed data matrix was further exported into SIMCA-P+^{TM} software (Umetrics, Kinnelon, NJ), transformed by Pareto scaling and then analyzed by principal components analysis (PCA). Major latent variables in the data matrix were described in a scores scatter plot of multivariate model. The potential chemical changes after IPL treatment was identified by analyzing ions contributing to the principal components and to the separation of sample groups in the loadings scatter plot. The chemicals' identity was identified by accurate mass measurement, elemental composition analysis, database search (Metlin, http://metlin.scripps.edu/; UniProt http://www.uniprot.org/), PEAKS Studio 8 (Bioinformatics Solutions Inc., Waterloo, ON, Canada), fragmentation, and comparison with authentic standards if possible.

3.2.8 Marker quantification

To quantify amino acids, and markers of interest, the ratio between the peak area of each amino acid and the peak area of internal standard was calculated and fitted with a standard curve using QuanLynx^{TM} software (Waters).

3.2.9 Statistical analysis

Statistical analysis was performed by one-way ANOVA and Turkey – Kramer comparison test using the GraphPad Prism 6 (GraphPad Software, La Jolla, CA, US). Significance is considered if $P<0.05$.

3.3 Results

3.3.1 Color of NFDM after IPL treatment

Color is a quality parameter during manufacturing of NFDM. The color of non-treated and IPL-treated NFDM was measured by colorimeter and recorded as CIE $L^*a^*b^*$ color space (Figure 3.1). One-way ANOVA and Turkey-Kramer comparison test was performed to determine the statistical significance of the changes. Total color difference was calculated and recorded as ΔE^*_{ab} (Figure 3.1).

Comparing to control (non-treated) NFDM, all IPL-treated samples experiences significant color shift in L^*, a^*, and b^* dimension ($p < 0.05$). The L^* value was significant lowered after IPL treatments, with control scored 90.30, illustrating a shift towards less overall whiteness. The a^* value was elevated from -3.59 to -0.53 after 4 passes. With a^* value being negative, the treated NFDM still fell in the dimension of green and shifted towards less green. The b^* value significantly dropped after 1 pass of IPL treatment from 12.02 to 9.46, showing a shift towards less yellow. Total color change reached 3.70 upon 1 pass and further escalated to 6.11 after 4 passes.

3.3.2 Amino acid profile of NFDM after IPL treatment

Milk protein contains all essential amino acids for human needs. To analyze the amino acids, the NFDM was first hydrolyzed with acid by microwave-assisted digestion, then derivatized with dansyl chloride for detection of amino-containing compounds by LC-MS. Tryptophan, methionine, and arginine were degraded during acid hydrolysis and hence were not quantified. The other amino acids profile remained unchanged after IPL treatment (Figure 3.2).

3.3.3 Chemometric investigation of IPL-elicited changes in NFDM

In order to investigate the chemical changes induced by IPL, the treated NFDM, along with control (non-treated), were extracted and examined through LC-MS based chemometric analysis. Multivariate data analysis was applied to analyze the data acquired from LC-MS. Principal component analysis (PCA) of the data obtained from polar fraction of NFDM extraction through a BEH C18 column followed by electron spray ionization and QTof mass spectrometry in positive detection mode achieved the clearest separation and grouping effect. As shown by the scores plot, IPL treatment dependent separation of non-treated control and IPL treated samples were observed in a PCA model, suggesting that the IPL treatment altered the NFDM chemical profile in a dose-dependent pattern (Figure 3.3A). The separation of non-treated and treated samples occurred along the first component of the model. Subsequently, the markers associated with control and 4-pass IPL treatment were identified in the loadings plot of PCA model, and their chemical identities were defined by the elemental composition analysis, database search, MSMS fragmentation, and confirmation by authentic standards. As shown in the loadings plot (Figure 3.3B), riboflavin and pantothenic acid are the nutrients that appeared to be degraded by IPL treatment and had higher concentration in non-treated NFDM. Several peptides were identified as IPL-responsive markers and were only found in IPL-treated NFDM.

3.3.3.1 Structural identification of IPL-responsive markers

The structures of the markers affected by IPL treatment was determined by multiple approaches. For example, the riboflavin and pantothenic acid were elucidated by analyzing the fragments in positive-mode MSMS fragmentograms. Comparison with

authentic standards of riboflavin and pantothenic acid were performed to confirm the identity of riboflavin and pantothenic acid. The preliminary amino acid composition of the peptides was firstly obtained by database search. Then the MSMS spectra were analyzed by PEAKS Studio 8.5 (Bioinformatics Solutions Inc., Waterloo, ON, Canada). The identified primary structure of peptides were aligned with milk protein primary structure based on UniProt peptide search (http://www.uniprot.org/). Two peptides were identified: H-Pro-Leu-Trp-OH and H-Pro-Ile-Ile-Val-OH, originated from c-terminal of α_{S1}-casein and β-casein respectively.

3.3.3.2 Correlation of NFDM color and IPL-responsive markers

Influences of IPL treatment on color of NFDM was reflected by the markers contributing to the separation of all five groups in the partial least square analysis (PLS) model (Figure 3.4). As shown in the loadings plot of the PLS model, degradation of riboflavin is associated to the color shift in *L** and *b** value, which is the shift towards less white and less yellow. Peptides were associated with the shift in a* value, which is the shift towards less green.

3.4 Discussion

3.4.1 IPL mediated changes on NFDM quality

Non-fat dry milk was treated by IPL at 4 different doses. Targeted analysis was performed to evaluate the color and amino acid profile of NFDM after IPL treatment. LC-MS based untargeted chemometric analysis was performed to evaluate the overall changes elicited by IPL. It appears that IPL does not alter amino acid profile of NFDM. The nutritional value given by milk protein was retained.

Color, measured by colorimeter, revealed significant changes on the total color space as indicated by ΔE^*_{ab} of almost 6 after 4 passes (Figure 3.1 D). A noticeable change is defined when ΔE^*_{ab} exceeds 1.5 [64]. Such shift might be the result of riboflavin degradation. Riboflavin gives liquid whole milk greenness color [61]. IPL degraded riboflavin in NFDM and caused a color shift to less green (Figure 3.1 B). Meanwhile, the PLS model indicated that the formation of peptides was associated with a decreased total whiteness (L* value) and yellowness (b* value) (Figure 3.1 A and C, Figure 3.4). Previous study evaluated the color modification on flour and black pepper treated by pulsed light. A total color shift of 6.1 and 8.5 were observed when the system reached 2 log reduction [39]. In a separate study, with the current IPL system, Although the IPL altered the color of milk powder, the capacity of its disinfection effect remains effective and promising [158]. Additionally, this change of color does not necessarily impact the proceeding manufacture of processed foods. NFDM is widely used as ingredient in producing processed food, including animal feed, meat and seafood products, baking, and beverages [156]. The influence on these processed products requires individual examination. Additionally, the measurement of colorimeter is different from human eye perception as the instruments pick up subtle changes that may not be apparent for human eye sight [159]. In a separate sensory study, trained sensory panelists examined the change on the appearance of NFDM. The sensory study represents the perception from consumers' point of view, and the result might be different from the instrumental measurement.

A PCA model based on untargeted LC-MS data revealed the formation of 7 peptides in NFDM after IPL treatment. Two of the peptides were identified as H-Pro-Leu-Trp-OH

and H-Pro-Ile-Ile-Val-OH from milk casein proteins. These two are the c-terminal sequences of α_{S1}-casein and β-casein, cleaved off from adjacent methionine and phenylalanine respectively. This result could be the photolysis of peptide bonds facilitated by UV irradiation. The three aromatic amino acids, phenylalanine, tryptophan, and tyrosine, absorb UV of 260-290 nm [160]. Excited aromatic side chains releases free electron, which can be transferred to the disulfide bridge in the protein and lead to its reduction [161]. The disassociated disulfide bond is reflected by the formation of H-Pro-Leu-Trp-OH as it was adjacent to methionine in α_{S1}-casein. In addition to aromatic amino acids, peptide bonds also absorbs UV at 190-230 nm, which is included in the IPL range [162]. However, this potential alteration in the advanced structure of protein does not affect the digestibility [70]. Meanwhile, the total amino acids profile in IPL-treated NFDM remained intact. Hence, the nutritional value of milk proteins was not influenced after IPL treatment.

3.4.2 Implications on development of IPL platform

Effect of IPL on NFDM was revealed by LC-MS based chemometric analysis. Although changes on color and chemical profile was revealed, the overall nutritional quality of milk proteins was intact. This result indicates potential modification for continuous development and upgrades of the existing IPL technology. The first strategy to further minimize the impact on the quality of NFDM is to manipulate the wavelength of light emitted by IPL. In previous chapter, the effect of IPL-mediated bactericidal events on *E. coli* was discussed. The IPL posed rapid and diminishing effect on membrane bound electron carrier, which ultimately led to cell death. These electron carriers, menaquinone-8, ubiquinone-8, and ubiquinol-8, were sensitive to near-UV (300-380 nm) and visible

light [129, 132]. But the absorbance of peptide bonds and aromatic amino acids are different, at 190-230 nm [162] and 250-290 nm respectively [160]. By enhancing the elicitation of near-UV light, corresponding to bactericidal effect, and removing the ranges influential to milk protein, the performance of IPL system might be improved.

Meanwhile, LC-MS based chemometrics can be applied to continuously monitor and compare the chemical changes in NFDM after IPL treatment. Current LC-MS method with pre-column extraction can effectively distinguish the treated and untreated samples. Additionally, the chemical shift displayed a dose-dependent pattern (Figure 3.3 A), which can be used to compare the NFDM treated by different IPL doses. However, in order to evaluate the quality change of NFDM with further details, more functional tests are needed.

In United States, NFDM is used mostly as an ingredient in food manufacturing rather than being directly consumed [156]. Depending on the product, NFDM is used for a variety of purposes, including foaming stability, color development, flavor, and nutrition value [163]. IPL is designed to disinfect NFDM prior to incorporating into food manufacturing. For food manufacturers, it will be important to ensure the quality and consistency of the NFDM. Evaluating NFDM's functioning properties after IPL treatment is hence also important as examining the chemical changes. Examples of functioning tests include enzymatic digestibility test [70], solubility test [70], foaming capacity test [164], and shelf life study [165].

Figure 3.1 Color of non-treated and IPL-treated NFDM

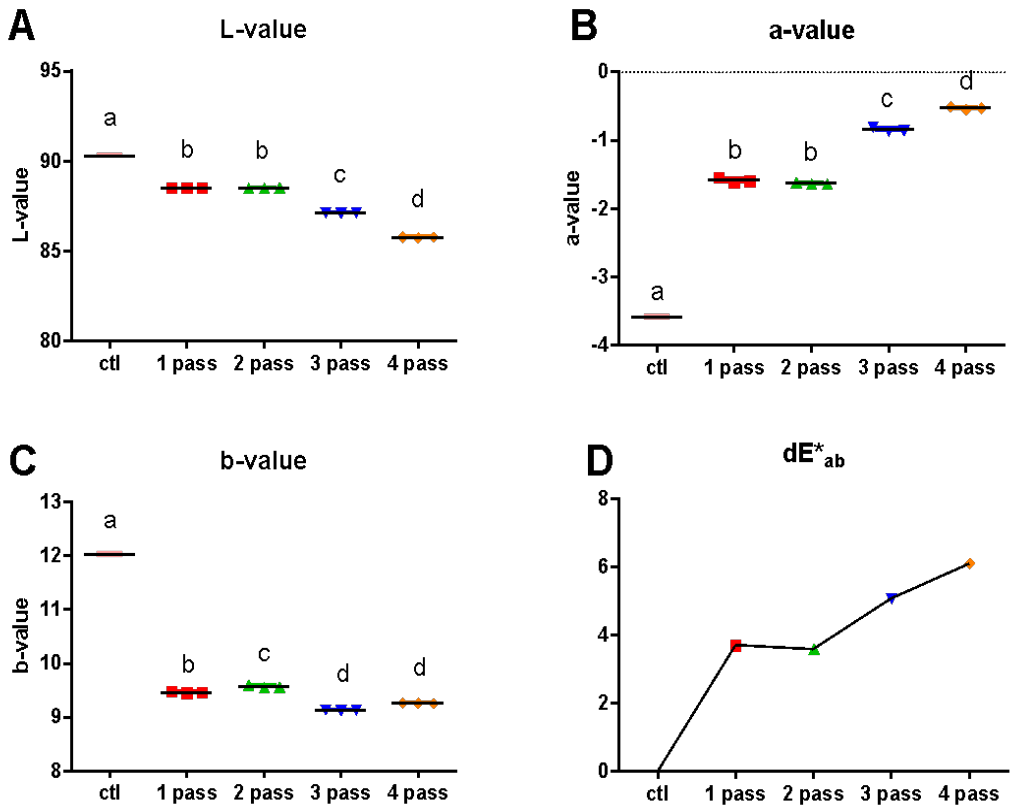

Figure 3.2 Amino acid profile of NFDM after IPL treatment

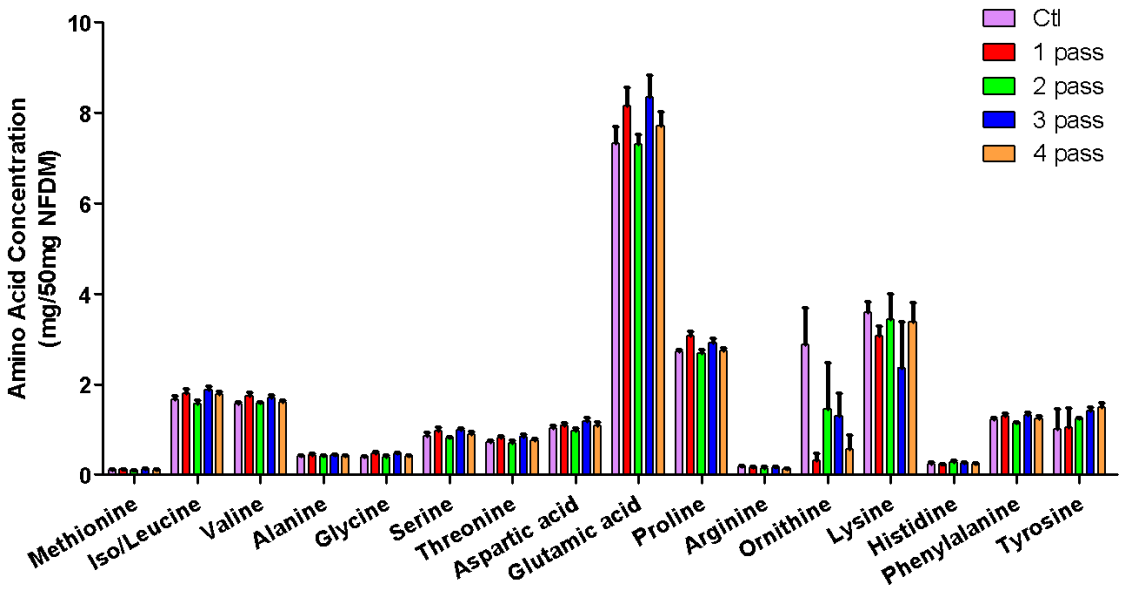

Figure 3.3 Effect of IPL treatment on NFDM chemical profile (Data from LC-MS analysis of the polar fraction of NFDM extraction by PCA model. The relations among non-treated control and IPL treated groups of NFDM are shown in the score plot. The markers correlating to the IPL treatment are labeled in the loadings plot. A: Scores plot of a PCA model on NFDM. B: Loadings plot of a PCA model on NFDM.)

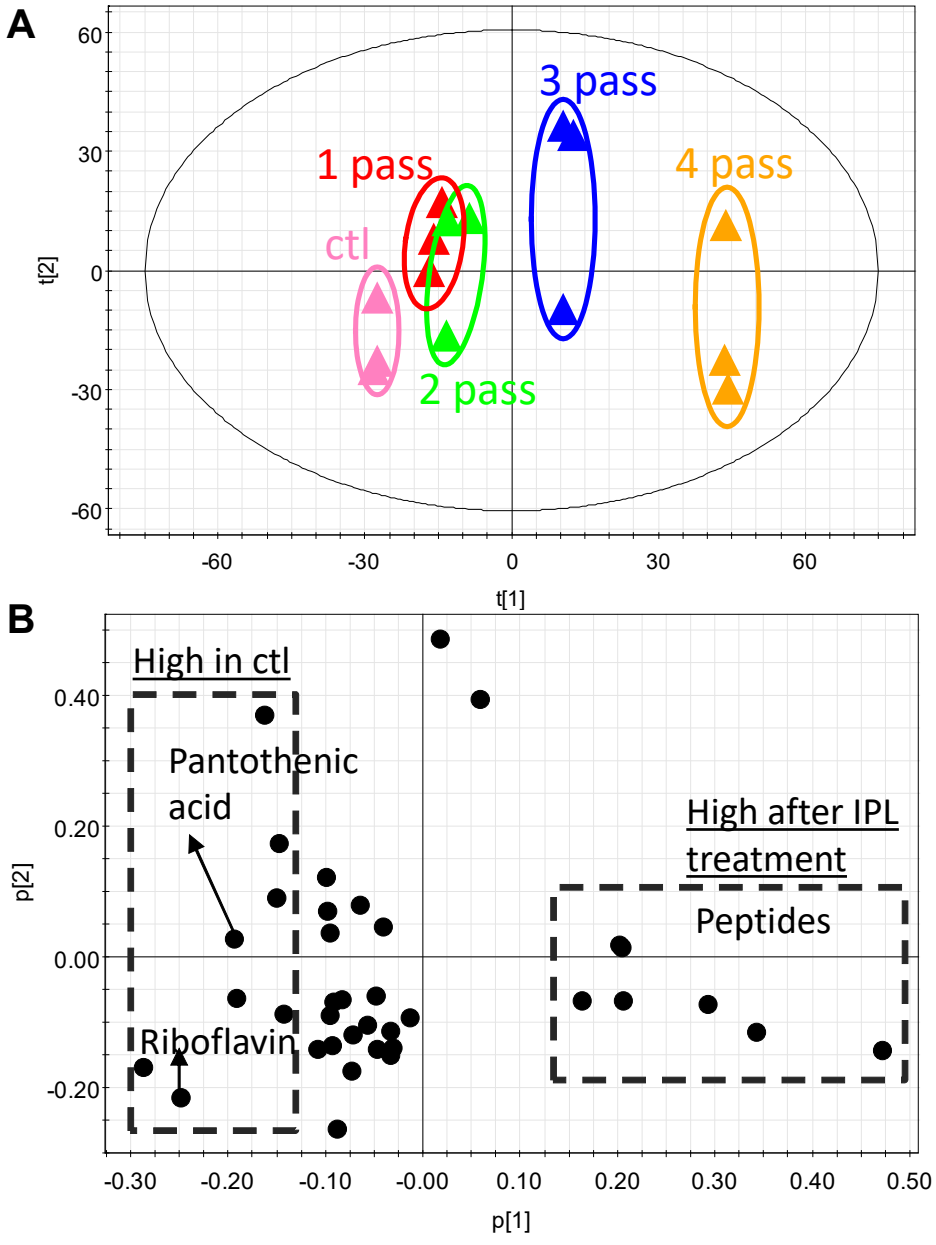

Figure 3.4 Loadings plot of PLS model, correlated with color change

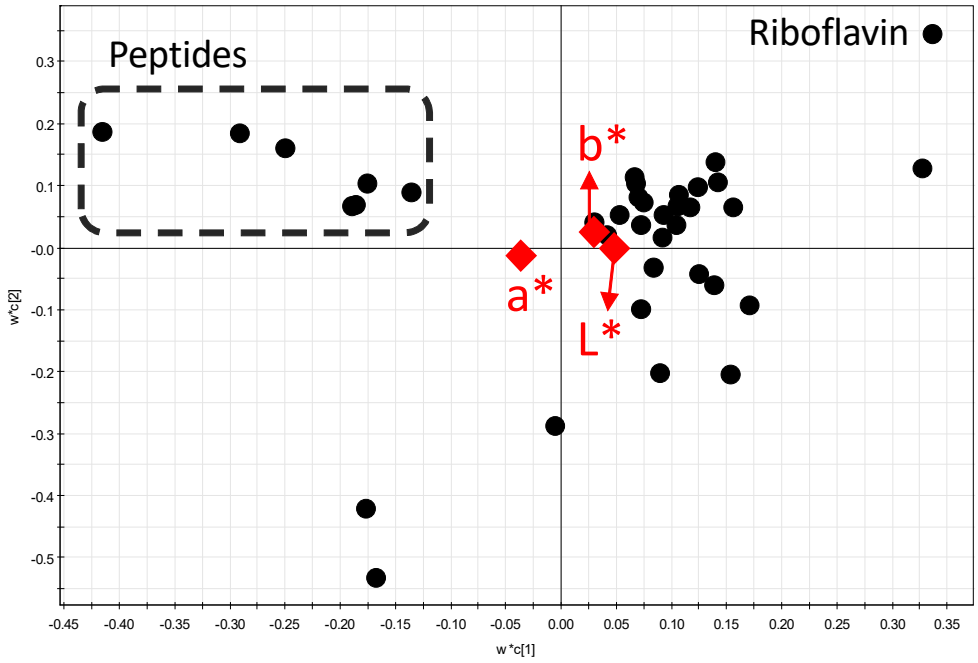

References

1. *National Outbreak Reporting System*, C.f.D.C.a. Prevention, Editor. 2017.
2. *List of Selected Multistate Foodborne Outbreak Investigations*, C.f.D.C.a. Prevention, Editor. 2018.
3. *Foodborne Illnesses: What You Need to Know*, U.S.F.D. Administration, Editor. 2018.
4. Scharff, R.L., *Economic burden from health losses due to foodborne illness in the United States.* Journal of food protection, 2012. **75**(1): p. 123-131.
5. Blount, Z.D., *The unexhausted potential of E. coli.* eLife, 2015. **4**: p. e05826.
6. Berg, H.C., *E. coli in Motion*. 2008: Springer Science & Business Media.
7. Sharma, V., et al., *Menaquinone (vitamin K2) biosynthesis: nucleotide sequence and expression of the menB gene from Escherichia coli.* Journal of bacteriology, 1992. **174**(15): p. 5057-5062.
8. Bélanger, L., et al., *Escherichia coli from animal reservoirs as a potential source of human extraintestinal pathogenic E. coli.* Pathogens and Disease, 2011. **62**(1): p. 1-10.
9. Kousta, M., et al., *Prevalence and sources of cheese contamination with pathogens at farm and processing levels.* Food control, 2010. **21**(6): p. 805-815.
10. *E. coli - Diagnosis & Treatment*. Diseases & Condition [Web] 2011 [cited 2018 May 31]; Available from: https://www.mayoclinic.org/diseases-conditions/e-coli/diagnosis-treatment/drc-20372064.
11. Endo, Y., et al., *Site of action of a Vero toxin (VT2) from Escherichia coli O157: H7 and of Shiga toxin on eukaryotic ribosomes.* The FEBS Journal, 1988. **171**(1‐2): p. 45-50.
12. Karpman, D., et al., *Apoptosis of renal cortical cells in the hemolytic-uremic syndrome: in vivo and in vitro studies.* Infection and immunity, 1998. **66**(2): p. 636-644.
13. Taguchi, T., et al., *Verotoxins induce apoptosis in human renal tubular epithelium derived cells.* Kidney international, 1998. **53**(6): p. 1681-1688.
14. Tarr, P.I., C.A. Gordon, and W.L. Chandler, *Shiga-toxin-producing Escherichia coli and haemolytic uraemic syndrome.* The Lancet, 2005. **365**(9464): p. 1073-1086.
15. Bogdan, J., J. Zarzyńska, and J. Pławińska-Czarnak, *Comparison of infectious agents susceptibility to photocatalytic effects of nanosized titanium and zinc oxides: a practical approach.* Nanoscale research letters, 2015. **10**(1): p. 309.
16. Cooper, G., *Cell Membranes*, in *The Cell: A Molecular Approach*. 2000, Sinauer Associates: Sunderland (MA).
17. Cronan Jr, J.E. and E.P. Gelmann, *Physical properties of membrane lipids: biological relevance and regulation.* Bacteriological reviews, 1975. **39**(3): p. 232.
18. Sousa, P.M., et al., *The aerobic respiratory chain of Escherichia coli: from genes to supercomplexes.* Microbiology, 2012. **158**(9): p. 2408-2418.
19. Dhar, S., et al., *Cell-wall recycling and synthesis in Escherichia coli and Pseudomonas aeruginosa - their role in the development of resistance.* J Med Microbiol, 2018. **67**(1): p. 1-21.

20. Reuter, M., et al., *Mechanosensitive channels and bacterial cell wall integrity: does life end with a bang or a whimper?* Journal of the Royal Society Interface, 2014. **11**(91): p. 20130850.
21. Giron, J.A., et al., *The flagella of enteropathogenic Escherichia coli mediate adherence to epithelial cells.* Mol Microbiol, 2002. **44**(2): p. 361-79.
22. Robicsek, A., G.A. Jacoby, and D.C. Hooper, *The worldwide emergence of plasmid-mediated quinolone resistance.* The Lancet infectious diseases, 2006. **6**(10): p. 629-640.
23. Bennett, P.M., *Plasmid encoded antibiotic resistance: acquisition and transfer of antibiotic resistance genes in bacteria.* British Journal of Pharmacology, 2008. **153**(Suppl 1): p. S347-S357.
24. Shapiro, R.S., *Antimicrobial-Induced DNA Damage and Genomic Instability in Microbial Pathogens.* PLoS Pathogens, 2015. **11**(3): p. e1004678.
25. Sanchez, S. and A.L. Demain, *Metabolic regulation and overproduction of primary metabolites.* Microbial biotechnology, 2008. **1**(4): p. 283-319.
26. Kurata, H., et al., *Integration of enzyme activities into metabolic flux distributions by elementary mode analysis.* BMC systems biology, 2007. **1**(1): p. 31.
27. Bren, A., et al., *Glucose becomes one of the worst carbon sources for E.coli on poor nitrogen sources due to suboptimal levels of cAMP.* Scientific Reports, 2016. **6**: p. 24834.
28. Bell, C. and A. Kyriakides, *Pathogenic Escherichia coli.* Foodborne pathogens, 2002: p. 279.
29. Gurtler, J.B., M.P. Doyle, and J.L. Kornacki, *The microbiological safety of low water activity foods and spices*. 2014, New York, NY: New York : Springer.
30. Chapman, K.W., H.T. Lawless, and K.J. Boor, *Quantitative Descriptive Analysis and Principal Component Analysis for Sensory Characterization of Ultrapasteurized Milk.* Journal of Dairy Science, 2001. **84**(1): p. 12-20.
31. Pereda, J., et al., *Effects of Ultra-High Pressure Homogenization on Microbial and Physicochemical Shelf Life of Milk.* Journal of Dairy Science, 2007. **90**(3): p. 1081-1093.
32. Zhao, J. and M. Cranston Peter, *Microbial decontamination of black pepper by ozone and the effect of the treatment on volatile oil constituents of the spice.* Journal of the Science of Food and Agriculture, 2006. **68**(1): p. 11-18.
33. Bononi, M., G. Quaglia, and F. Tateo, *Identification of ethylene oxide in herbs, spices and other dried vegetables imported into Italy.* Food Additives & Contaminants: Part A, 2014. **31**(2): p. 271-275.
34. Perry, J.J. and A.E. Yousef, *Decontamination of raw foods using ozone-based sanitization techniques.* Annual review of food science and technology, 2011. **2**: p. 281-298.
35. Lung, H.-M., et al., *Microbial decontamination of food by electron beam irradiation.* Trends in Food Science & Technology, 2015. **44**(1): p. 66-78.
36. Sudarmadji, S. and M. Urbain W, *Flavor sensitivity of selected animal protein foods to gamma radiation.* Journal of Food Science, 2006. **37**(5): p. 671-672.
37. Farkas, J. and C. Mohácsi-Farkas, *History and future of food irradiation.* Trends in Food Science & Technology, 2011. **22**(2-3): p. 121-126.

38. Guerrero-Beltr·n, J.A. and G.V. Barbosa-C·novas, *Advantages and Limitations on Processing Foods by UV Light.* Food Science and Technology International, 2004. **10**(3): p. 137-147.
39. Fine, F. and P. Gervais, *Efficiency of pulsed UV light for microbial decontamination of food powders.* Journal of food protection, 2004. **67**(4): p. 787-792.
40. Santillana Farakos, S.M. and J.F. Frank, *Challenges in the Control of Foodborne Pathogens in Low-Water Activity Foods and Spices*, in *The Microbiological Safety of Low Water Activity Foods and Spices*, J.B. Gurtler, M.P. Doyle, and J.L. Kornacki, Editors. 2014, Springer New York: New York, NY. p. 15-34.
41. Beuchat, L.R., et al., *Low–water activity foods: increased concern as vehicles of foodborne pathogens.* Journal of Food Protection, 2013. **76**(1): p. 150-172.
42. Beuchat, L., et al., *Persistence and survival of pathogens in dry foods and dry food processing environments.* 2011.
43. Asao, T., et al., *An extensive outbreak of staphylococcal food poisoning due to low-fat milk in Japan: estimation of enterotoxin A in the incriminated milk and powdered skim milk.* Epidemiology and infection, 2003. **130**(1): p. 33.
44. Simmons, B.P., et al., *Enterobacter sakazakii infections in neonates associated with intrinsic contamination of a powdered infant formula.* Infect Control Hosp Epidemiol, 1989. **10**(9): p. 398-401.
45. Little, C., R. Omotoye, and R. Mitchell, *The microbiological quality of ready-to-eat foods with added spices.* International Journal of Environmental Health Research, 2003. **13**(1): p. 31-42.
46. Gieraltowski, L., et al., *Notes from the field: multistate outbreak of Escherichia coli O157: H7 infections linked to dough mix—United States, 2016.* MMWR. Morbidity and mortality weekly report, 2017. **66**(3): p. 88.
47. Bhavya, M.L. and H. Umesh Hebbar, *Pulsed light processing of foods for microbial safety.* Food Quality and Safety, 2017. **1**(3): p. 187-202.
48. Gomez-Lopez, V.M., et al., *Pulsed light for food decontamination: a review.* Trends in food science & technology, 2007. **18**(9): p. 464-473.
49. Palgan, I., et al., *Effectiveness of High Intensity Light Pulses (HILP) treatments for the control of Escherichia coli and Listeria innocua in apple juice, orange juice and milk.* Food Microbiol, 2011. **28**(1): p. 14-20.
50. Elmnasser, N., et al., *Pulsed-light system as a novel food decontamination technology: a review.* Can J Microbiol, 2007. **53**(7): p. 813-21.
51. Pereira, R.N. and A.A. Vicente, *Environmental impact of novel thermal and non-thermal technologies in food processing.* Food Research International, 2010. **43**(7): p. 1936-1943.
52. Choi, M.-S., et al., *Nonthermal sterilization of Listeria monocytogenes in infant foods by intense pulsed-light treatment.* Journal of Food Engineering, 2010. **97**(4): p. 504-509.
53. Oms-Oliu, G., O. Martín-Belloso, and R. Soliva-Fortuny, *Pulsed light treatments for food preservation. A review.* Food and Bioprocess Technology, 2008. **3**(1): p. 13.

54. *General Specifications for Dairy Plants Approved for USDA Inspection and Grading Service*, USDA, Editor. 2012.
55. *United States Standards for Grades of Nonfat Dry Milk (Spray Process)*, U.S.D.o.H.a.H.S.a.U.S.D.o. Agriculture., Editor. 2001.
56. Fox, P.F., et al., *Dairy chemistry and biochemistry*. Second edition.. ed. 2015, Cham: Cham : Springer.
57. Wong, N.P., *Fundamentals of dairy chemistry*. 3rd ed.. ed. 1988, New York: New York : Van Nostrand Reihold Co.
58. Haug, A., A.T. Høstmark, and O.M. Harstad, *Bovine milk in human nutrition–a review.* Lipids in health and disease, 2007. **6**(1): p. 25.
59. Powell, J., *The sensory and analytical analyses of nonfat milk formulations: Stability to light oxidation and pasteurization*. 2001, Virginia Tech.
60. Walstra, P. and R. Jenness, *Dairy chemistry & physics*. 1984: John Wiley & Sons.
61. Y.H., H., *Dairy science and technology handbook.* 1993.
62. Abdalla, A., K. Smith, and J. Lucey, *Physical Properties of Nonfat Dry Milk and Skim Milk Powder.* International Journal of Dairy Science, 2017. **12**: p. 149-154.
63. Chugh, A., et al., *Change in Color and Volatile Composition of Skim Milk Processed with Pulsed Electric Field and Microfiltration Treatments or Heat Pasteurization (†).* Foods, 2014. **3**(2): p. 250-268.
64. Cserhalmi, Z., et al., *Study of pulsed electric field treated citrus juices.* Innovative Food Science & Emerging Technologies, 2006. **7**(1-2): p. 49-54.
65. Walkling-Ribeiro, M., et al., *The impact of thermosonication and pulsed electric fields on Staphylococcus aureus inactivation and selected quality parameters in orange juice.* Food and Bioprocess Technology, 2009. **2**(4): p. 422.
66. Grigioni, G., et al., *Color changes of milk powder due to heat treatments and season of manufacture.* CYTA-Journal of Food, 2007. **5**(5): p. 335-339.
67. Ruas-Madiedo, P., J. Hugenholtz, and P. Zoon, *An overview of the functionality of exopolysaccharides produced by lactic acid bacteria.* International Dairy Journal, 2002. **12**(2-3): p. 163-171.
68. Choe, E., R. Huang, and D.B. Min, *Chemical reactions and stability of riboflavin in foods.* Journal of Food Science, 2005. **70**(1).
69. Lee, K., M. Jung, and S. Kim, *Effects of ascorbic acid on the light-induced riboflavin degradation and color changes in milks.* Journal of agricultural and food chemistry, 1998. **46**(2): p. 407-410.
70. Scheidegger, D., et al., *Protein oxidative changes in whole and skim milk after ultraviolet or fluorescent light exposure.* Journal of dairy science, 2010. **93**(11): p. 5101-5109.
71. Dalsgaard, T.K., et al., *Changes in structures of milk proteins upon photo-oxidation.* Journal of agricultural and food chemistry, 2007. **55**(26): p. 10968-10976.
72. Siddique, M.A.B., et al., *Effect of pulsed light treatment on structural and functional properties of whey protein isolate.* Food Research International, 2016. **87**: p. 189-196.

73. Thomsen, M.K., et al., *Temperature effect on lactose crystallization, maillard reactions, and lipid oxidation in whole milk powder.* J Agric Food Chem, 2005. **53**(18): p. 7082-90.
74. Jones, A., C. Tier, and J. Wilkins, *Analysis of the Maillard reaction products of ß-lactoglobulin and lactose in skimmed milk powder by capillary electrophoresis and electrospray mass spectrometry.* Journal of Chromatography A, 1998. **822**(1): p. 147-154.
75. Sell, D.R., *Ageing promotes the increase of early glycation Amadori product as assessed by ϵ-N-(2-furoylmethyl)-l-lysine (furosine) levels in rodent skin collagen: The relationship to dietary restriction and glycoxidation.* Mechanisms of Ageing and Development, 1997. **95**(1): p. 81-99.
76. Li, Y., et al., *Qualitative and quantitative analysis of furosine in fresh and processed ginsengs.* Journal of Ginseng Research, 2018. **42**(1): p. 21-26.
77. Morales, F. and M. Van Boekel, *A study on advanced Maillard reaction in heated casein/sugar solutions: colour formation.* International Dairy Journal, 1998. **8**(10-11): p. 907-915.
78. WATANABE, F., et al., *Effect of light-induced riboflavin degradation on the loss of cobalamin in milk.* Journal of Home Economics of Japan, 2000. **51**(3): p. 231-234.
79. Furuya, E. and J. Warthesen, *Influence of initial riboflavin content on retention in pasta during photodegradation and cooking.* Journal of Food Science, 1984. **49**(4): p. 984-986.
80. Kato, Y., K. Uchida, and S. Kawakishi, *Aggregation of collagen exposed to UVA in the presence of riboflavin: a plausible role of tyrosine modification.* Photochemistry and photobiology, 1994. **59**(3): p. 343-349.
81. Silva, E., A.M.a. Edwards, and D. Pacheco, *Visible light-induced photooxidation of glucose sensitized by riboflavin.* The Journal of nutritional biochemistry, 1999. **10**(3): p. 181-185.
82. Whited, L., et al., *Vitamin A degradation and light-oxidized flavor defects in milk.* Journal of dairy science, 2002. **85**(2): p. 351-354.
83. Gates, S.C. and C.C. Sweeley, *Quantitative metabolic profiling based on gas chromatography.* Clinical chemistry, 1978. **24**(10): p. 1663-1673.
84. Gowda, G.A.N. and D. Djukovic, *Overview of Mass Spectrometry-Based Metabolomics: Opportunities and Challenges.* Methods in molecular biology (Clifton, N.J.), 2014. **1198**: p. 3-12.
85. Esbensen, K. and P. Geladi, *The start and early history of chemometrics: Selected interviews. Part 2.* Journal of Chemometrics, 1990. **4**(6): p. 389-412.
86. Schlager, K.J. and T.L. Ruchti. *Overview of chemometrics*. in *Ultrasensitive Instrumentation for DNA Sequencing and Biochemical Diagnostics*. 1995. International Society for Optics and Photonics.
87. Kumar, N., et al., *Chemometrics tools used in analytical chemistry: An overview.* Talanta, 2014. **123**: p. 186-199.
88. Fiehn, O., *Metabolomics — the link between genotypes and phenotypes.*, in *Functional Genomics.*, C. Town, Editor. 2002, Springer, Dordrecht. p. 155-171.

89. Teng, Q., et al., *A direct cell quenching method for cell-culture based metabolomics.* Metabolomics, 2009. **5**(2): p. 199.
90. Cevallos-Cevallos, J.M., et al., *Metabolomic analysis in food science: a review.* Trends in Food Science & Technology, 2009. **20**(11-12): p. 557-566.
91. Lu, Y., D. Yao, and C. Chen, *2-Hydrazinoquinoline as a derivatization agent for LC-MS-based metabolomic investigation of diabetic ketoacidosis.* Metabolites, 2013. **3**(4): p. 993-1010.
92. Jia, S., et al., *Simultaneous determination of 23 amino acids and 7 biogenic amines in fermented food samples by liquid chromatography/quadrupole time-of-flight mass spectrometry.* Journal of Chromatography A, 2011. **1218**(51): p. 9174-9182.
93. Dunn, W.B. and D.I. Ellis, *Metabolomics: current analytical platforms and methodologies.* TrAC Trends in Analytical Chemistry, 2005. **24**(4): p. 285-294.
94. Weybright, P., et al., *Gradient, high‐resolution, magic angle spinning 1H nuclear magnetic resonance spectroscopy of intact cells.* Magnetic resonance in medicine, 1998. **39**(3): p. 337-345.
95. Pan, Z. and D. Raftery, *Comparing and combining NMR spectroscopy and mass spectrometry in metabolomics.* Analytical and bioanalytical chemistry, 2007. **387**(2): p. 525-527.
96. Deng, C., X. Zhang, and N. Li, *Investigation of volatile biomarkers in lung cancer blood using solid-phase microextraction and capillary gas chromatography–mass spectrometry.* Journal of Chromatography B, 2004. **808**(2): p. 269-277.
97. Chen, C. and S. Kim, *LC-MS-based metabolomics of xenobiotic-induced toxicities.* Computational and structural biotechnology journal, 2013. **4**(5): p. 1-10.
98. Tautenhahn, R., et al., *An accelerated workflow for untargeted metabolomics using the METLIN database.* Nature biotechnology, 2012. **30**(9): p. 826-828.
99. Roberts, J.J. and D. Cozzolino, *An Overview on the Application of Chemometrics in Food Science and Technology—An Approach to Quantitative Data Analysis.* Food Analytical Methods, 2016. **9**(12): p. 3258-3267.
100. Capozzi, F. and A. Bordoni, *Foodomics: a new comprehensive approach to food and nutrition.* Genes Nutr, 2013. **8**(1): p. 1-4.
101. Herrero, M., et al., *Foodomics: MS-based strategies in modern food science and nutrition.* Mass Spectrom Rev, 2012. **31**(1): p. 49-69.
102. Gallo, M. and P. Ferranti, *The evolution of analytical chemistry methods in foodomics.* J Chromatogr A, 2016. **1428**: p. 3-15.
103. Metallo, C.M. and M.G.V. Heiden, *Understanding metabolic regulation and its influence on cell physiology.* Molecular cell, 2013. **49**(3): p. 388-398.
104. Cairns, R.A., I.S. Harris, and T.W. Mak, *Regulation of cancer cell metabolism.* Nat Rev Cancer, 2011. **11**(2): p. 85-95.
105. Zhang, A., et al., *Cell Metabolomics.* OMICS : a Journal of Integrative Biology, 2013. **17**(10): p. 495-501.
106. Wright, G.D., *On the Road to Bacterial Cell Death.* Cell, 2007. **130**(5): p. 781-783.

107. Kohanski, M.A., et al., *A common mechanism of cellular death induced by bactericidal antibiotics.* Cell, 2007. **130**(5): p. 797-810.
108. Wang, T.J., et al., *Metabolite profiles and the risk of developing diabetes.* Nature medicine, 2011. **17**(4): p. 448-453.
109. Mashego, M.R., et al., *Microbial metabolomics: past, present and future methodologies.* Biotechnology Letters, 2007. **29**(1): p. 1-16.
110. Chen, C., F.J. Gonzalez, and J.R. Idle, *LC-MS-based metabolomics in drug metabolism.* Drug Metab Rev, 2007. **39**(2-3): p. 581-97.
111. Lu, Y. and C. Chen, *Metabolomics: Bridging Chemistry and Biology in Drug Discovery and Development.* Current Pharmacology Reports, 2017. **3**(1): p. 16-25.
112. Armitage, E.G. and C. Barbas, *Metabolomics in cancer biomarker discovery: Current trends and future perspectives.* Journal of Pharmaceutical and Biomedical Analysis, 2014. **87**: p. 1-11.
113. Hasunuma, T., et al., *Metabolic pathway engineering based on metabolomics confers acetic and formic acid tolerance to a recombinant xylose-fermenting strain of Saccharomyces cerevisiae.* Microbial Cell Factories, 2011. **10**(1): p. 2.
114. Rice, R.G. and D.M. Graham, *US FDA regulatory approval of ozone as an antimicrobial agent–what is allowed and what needs to be understood.* Ozone News, 2001. **29**(5): p. 22-31.
115. *Irradiation in the production, processing, and handling of food*, in *21*, U.S.F.D. Administration, Editor. 2017.
116. Groh, C.D., D.W. MacPherson, and D.J. Groves, *Effect of heat on the sterilization of artificially contaminated water.* Journal of travel medicine, 1996. **3**(1): p. 11-13.
117. Li, M., J.H. Qu, and Y.Z. Peng, *Sterilization of Escherichia coli cells by the application of pulsed magnetic field.* J Environ Sci (China), 2004. **16**(2): p. 348-52.
118. Perni, S., G. Shama, and M.G. Kong, *Cold atmospheric plasma disinfection of cut fruit surfaces contaminated with migrating microorganisms.* Journal of food protection, 2008. **71**(8): p. 1619-1625.
119. Laroussi, M., et al., *Images of biological samples undergoing sterilization by a glow discharge at atmospheric pressure.* IEEE Transactions on plasma science, 1999. **27**(1): p. 34-35.
120. Kamihira, M., M. Taniguchi, and T. Kobayashi, *Sterilization of microorganisms with supercritical carbon dioxide.* Agricultural and Biological Chemistry, 1987. **51**(2): p. 407-412.
121. Bucheli-Witschel, M., C. Bassin, and T. Egli, *UV-C inactivation in Escherichia coli is affected by growth conditions preceding irradiation, in particular by the specific growth rate.* J Appl Microbiol, 2010. **109**(5): p. 1733-44.
122. Takeshita, K., et al., *Damage of yeast cells induced by pulsed light irradiation.* International Journal of Food Microbiology, 2003. **85**(1): p. 151-158.
123. Kramer, B. and P. Muranyi, *Effect of pulsed light on structural and physiological properties of Listeria innocua and Escherichia coli.* Journal of applied microbiology, 2014. **116**(3): p. 596-611.

124. Cheigh, C.-I., et al., *Comparison of intense pulsed light-and ultraviolet (UVC)-induced cell damage in Listeria monocytogenes and Escherichia coli O157: H7.* Food Control, 2012. **25**(2): p. 654-659.
125. Kim, S., et al., *Bacterial inactivation in water, DNA strand breaking, and membrane damage induced by ultraviolet-assisted titanium dioxide photocatalysis.* Water research, 2013. **47**(13): p. 4403-4411.
126. Loughlin, A.F., et al., *An ion exchange liquid chromatography/mass spectrometry method for the determination of reduced and oxidized glutathione and glutathione conjugates in hepatocytes.* Journal of Pharmaceutical and Biomedical Analysis, 2001. **26**(1): p. 131-142.
127. Aussel, L., et al., *Biosynthesis and physiology of coenzyme Q in bacteria.* Biochimica et Biophysica Acta (BBA) - Bioenergetics, 2014. **1837**(7): p. 1004-1011.
128. Søballe, B. and R.K. Poole, *Microbial ubiquinones: multiple roles in respiration, gene regulation and oxidative stress management.* Microbiology, 1999. **145**(8): p. 1817-1830.
129. Madden, J.J., D.T. Boatwright, and J. Jagger, *Action spectra for modification of Escherichia Coli B/r menaquinone by near-ultraviolet and visible radiations (313-578 nm)*.* Photochemistry and Photobiology, 1981. **33**(3): p. 305-311.
130. Villalba, J.M., F.L. Crane, and P. Navas, *Antioxidative role of ubiquinone in the animal plasma membrane*, in *Plasma Membrane Redox Systems and their Role in Biological Stress and Disease*, H. Asard, A. Bérczi, and R.J. Caubergs, Editors. 1998, Springer Netherlands: Dordrecht. p. 247-265.
131. Dunlap, W.C., A. Fujisawa, and Y. Yamamoto, *UV radiation increases the reduced coenzyme Q ratio in marine bacteria.* Redox report, 2002. **7**(5): p. 320-323.
132. Werbin, H., B.D. Lakchaura, and J. Jagger, *Near-ultraviolet modification of Escherichia Coli B Ubiquinone in vivo and in vitro.* Photochemistry and photobiology, 1974. **19**(5): p. 321-328.
133. MacLeod, R.A., P. Thurman, and H. Rogers, *Comparative transport activity of intact cells, membrane vesicles, and mesosomes of Bacillus licheniformis.* Journal of bacteriology, 1973. **113**(1): p. 329-340.
134. Newton, N., G. Cox, and F. Gibson, *The function of menaquinone (vitamin K2) in Escherichia coli K-12.* Biochimica et Biophysica Acta (BBA)-General Subjects, 1971. **244**(1): p. 155-166.
135. Booth, I.R. and C.F. Higgins, *Enteric bacteria and osmotic stress: Intracellular potassium glutamate as a secondary signal of osmotic stress?* FEMS Microbiology Letters, 1990. **75**(2): p. 239-246.
136. Wood, J.M., *Bacterial osmoregulation: a paradigm for the study of cellular homeostasis.* Annual review of microbiology, 2011. **65**: p. 215-238.
137. Yuan, W., et al., *Hypochlorous acid converts the γ-glutamyl group of glutathione disulfide to 5-hydroxybutyrolactam, a potential marker for neutrophil activation.* Journal of Biological Chemistry, 2009. **284**(39): p. 26908-26917.
138. Drazic, A., et al., *Metabolic response of Escherichia coli upon treatment with hypochlorite at sub-lethal concentrations.* PloS one, 2015. **10**(5): p. e0125823.

139. Carper, S., et al., *Spermidine acetylation in response to a variety of stresses in Escherichia coli.* Journal of Biological Chemistry, 1991. **266**(19): p. 12439-12441.
140. Edgar, J.R. and R.M. Bell, *Biosynthesis in Escherichia coli fo sn-glycerol 3-phosphate, a precursor of phospholipid.* Journal of Biological Chemistry, 1978. **253**(18): p. 6348-6353.
141. Mráček, T., Z. Drahota, and J. Houštěk, *The function and the role of the mitochondrial glycerol-3-phosphate dehydrogenase in mammalian tissues.* Biochimica et Biophysica Acta (BBA) - Bioenergetics, 2013. **1827**(3): p. 401-410.
142. Henderson, J.R., et al., *Direct, real-time monitoring of superoxide generation in isolated mitochondria.* Free radical research, 2009. **43**(9): p. 796-802.
143. Bosshard, F., et al., *The respiratory chain is the cell's Achilles' heel during UVA inactivation in Escherichia coli.* Microbiology, 2010. **156**(7): p. 2006-2015.
144. Peralta, D.R., et al., *Enterobactin as part of the oxidative stress response repertoire.* PloS one, 2016. **11**(6): p. e0157799.
145. Adler, C., et al., *The alternative role of enterobactin as an oxidative stress protector allows Escherichia coli colony development.* PloS one, 2014. **9**(1): p. e84734.
146. Pérez-González, A., A. Galano, and J.R. Alvarez-Idaboy, *Dihydroxybenzoic acids as free radical scavengers: mechanisms, kinetics, and trends in activity.* New Journal of Chemistry, 2014. **38**(6): p. 2639-2652.
147. Forkert, P.-G., et al., *Diminished CYP2E1 expression and formation of 2-S-glutathionyl acetate, a glutathione conjugate derived from 1, 1-dichloroethylene epoxide, in murine lung tumors.* Drug metabolism and disposition, 1999. **27**(1): p. 68-73.
148. Rathinasamy, T. and L. Augenstein, *Photochemical yields in ribonuclease and oxidized glutathione irradiated at different wavelengths in the ultraviolet.* Biophysical journal, 1968. **8**(11): p. 1275-1287.
149. Kruger, N.J. and A. von Schaewen, *The oxidative pentose phosphate pathway: structure and organisation.* Current opinion in plant biology, 2003. **6**(3): p. 236-246.
150. Kuehne, A., et al., *Acute activation of oxidative pentose phosphate pathway as first-line response to oxidative stress in human skin cells.* Molecular cell, 2015. **59**(3): p. 359-371.
151. Yan, M. and J.D. Gralla, *Multiple ATP-dependent steps in RNA polymerase II promoter melting and initiation.* The EMBO Journal, 1997. **16**(24): p. 7457-7467.
152. Martin, I.V. and S.A. MacNeill, *ATP-dependent DNA ligases.* Genome Biol, 2002. **3**(4): p. Reviews3005.
153. Truglio, J.J., et al., *Prokaryotic nucleotide excision repair: the UvrABC system.* Chemical reviews, 2006. **106**(2): p. 233-252.
154. Leuschner, R.G.K. and P.J. Lillford, *Investigation of bacterial spore structure by high resolution solid-state nuclear magnetic resonance spectroscopy and transmission electron microscopy.* International Journal of Food Microbiology, 2001. **63**(1): p. 35-50.

155. Bottone, E.J., *Bacillus cereus, a volatile human pathogen.* Clin Microbiol Rev, 2010. **23**(2): p. 382-98.
156. Hunter, C.J. and J.F. Bean, *Cronobacter: an emerging opportunistic pathogen associated with neonatal meningitis, sepsis and necrotizing enterocolitis.* Journal Of Perinatology, 2013. **33**: p. 581.
157. Moreira, M.R., et al., *Effects of pulsed light treatments and pectin edible coatings on the quality of fresh‐cut apples: a hurdle technology approach.* Journal of the Science of Food and Agriculture, 2017. **97**(1): p. 261-268.
158. Chen, D., et al., *Effects of intense pulsed light on Cronobacter sakazakii inoculated in non-fat dry milk.* Journal of Food Engineering, 2018. **238**: p. 178-187.
159. Minolta, K., *Precise color communication.* Mahwah, NJ: Konica Minolta Sensing, Inc, 1998.
160. Bensasson, R., E. Land, and T. Truscott, *Pulse radiolysis and flash photolysis: Contributions to the chemistry of biology and medicine*. 1983, Pergamon Press, Oxford.
161. Neves-Petersen, M.T., et al., *Flash photolysis of cutinase: identification and decay kinetics of transient intermediates formed upon UV excitation of aromatic residues.* Biophysical journal, 2009. **97**(1): p. 211-226.
162. Goldfarb, A.R., L.J. Saidel, and E. Mosovich, *The ultraviolet absorption spectra of proteins.* Journal of Biological Chemistry, 1951. **193**: p. 397-404.
163. *Using milk powder*. U.S. Dairy Products [Web]; Available from: http://www.thinkusadairy.org/products/milk-powders/using-milk-powder.
164. Farrag, A., *Emulsifying and foaming properties of whey protein concentrates in the presence of some carbohydrates.* International Journal of Dairy Science, 2008. **3**(1): p. 20-28.
165. Mohamed, Z., et al., *Monitoring Shelf Life of Pasteurized Whole Milk Under Refrigerated Storage Conditions: Predictive Models for Quality Loss.* Journal of Food Science, 2018. **83**(2): p. 409-418.